AN ANALYSIS OF DENDRITIC COOPERATIVITY IN PROTEIN HYDROLYSIS

by

Jacob Webb O'Dell

A thesis submitted in partial fulfillment
of the requirements for the degree

of

Master of Science

in

Chemistry

MONTANA STATE UNIVERSITY
Bozeman, Montana

July 2005

APPROVAL

of a thesis submitted by

Jacob Webb O'Dell

This thesis has been read by each member of the thesis committee and has been found to be satisfactory regarding content, English usage, format, citations, bibliographic style, and consistency, and is ready for submission to the College of Graduate Studies.

Mary J. Cloninger

Approved for the Department of Chemistry and Biochemistry

David J. Singel

Approved for the College of Graduate Studies

Joseph J. Fedock

STATEMENT OF PERMISSION TO USE

In presenting this thesis in partial fulfillment of the requirements for a master's degree at Montana State University, I agree that the Library shall make it available to borrowers under rules of the Library.

If I have indicated my intention to copyright this thesis by including a copyright notice page, copying is allowable only for scholarly purposes, consistent with "fair use" as prescribed in the U.S. Copyright Law. Requests for permission for extended quotation from or reproduction of this thesis in whole or in parts may be granted only by the copyright holder.

Jacob Webb O'Dell

July 14, 2005

To Heath, who never quit trying

ACKNOWLEDGEMENTS

First I have to thank Mary for putting with me far longer than any one person should have to and for all the years of NIH sponsored snowboarding. You've been an amazing mentor of life as well as science. I'll miss the heterocycles game and ethics lectures. Second I want to thank my family: Mom, Dad, Caleb, and Isaac in TN for their unwavering support. No matter where I go, I know that I have a home and people that I love to come back to. I want to thank my Grandma O'Dell for keeping my secrets and making sure I always had what I needed and spoiling me just because. Thanks to Zeke and Beavis for making sure I don't take myself to seriously. My research group has been incredible. Mark is responsible for adding at least a year to my time here, and I'll never be able to thank you enough. Nick has always been there when I needed him, a friend couldn't ask any more. Morgan, you're a dirty little beast. Dr. Eric Woller taught me the finer points of working the second shift. Lab wasn't as fun without you. Thanks to all other Cloninger group members. Bob Busse, you are the zen master because you don't know it. Thank you for all you taught me. I will miss you and Walt. Thanks to Mr. Jordan for letting us pitch the tipi on your place. Thanks to Specs, PBR, Booker Noe, Bridger Bowl, Ular the snow god, the Hauf, and Northern Lights for taking all my money. Lastly, thanks Heath. Kindred spirits are never far from one another, whether they know it or not.

TABLE OF CONTENTS

LIST OF TABLES

Table Page

LIST OF FIGURES

Figure Page

LIST OF FIGURES-CONTINUED

Figure Page

LIST OF FIGURES-CONTINUED

Figure Page

LIST OF SCHEMES

ABSTRACT

Catalysts are compounds that increase the rate of a chemical reaction by lowering the activation energy while not being permanently altered. Adding a catalyst to a reaction, while increasing the rate, complicates purification because the catalyst must be separated from the product(s) of the reaction. If the catalyst is a drastically different size than the product then seperation can be achieved as easily as filtering over a membrane. Dendrimers are becoming popular scaffolding for tethering catalysts. Attaching a catalyst to a dendrimer makes a bigger catalytic unit that is easily separated from reaction product(s) of similar size to the untethered catalyst. However, attaching a catalyst to a dendritic framework usually results in a decrease in the catalyst's activity.

Previous work reported that attaching three salicylic acid residues in close proximity to each other on a linear PPI polymer catalyzed the hydrolysis of the protein immunoglobulin G's peptide backbone. Attaching three salicylic acid residues at random locations on the polymer showed significantly less catalytic activity.

Salicylic acid functionalized generations 1-5 PPI dendrimers were synthesized and characterized. Rate enhancement of IgG hydrolysis by the functionalized dendrimers was studied with SDS-PAGE. Generation 5 salicylic acid functionalized PPI dendrimers catalyzed the hydrolysis of IgG while lower generations and 5-nitrosalicylic acid did not. Generation 5 salicylic acid functionalized dendrimers catalyzing IgG hydrolysis is another in a small number of examples of catalytic systems enhanced by dendritic scaffolding.

CHAPTER ONE

INTRODUCTION

Catalysis

Compounds that promote reactions without being altered are catalysts. Catalysts are indispensable in industry due to their inherent abilities to lower the activation energy of reactions and increase rates of product formation. Catalysts are divided into three basic classifications: heterogeneous, homogeneous, and biological (enzymatic). [1]

Heterogeneous catalysis is the direct result of the initial conception of catalysis by Berzelius in the 1830s.[2,3] Heterogeneous catalysts are defined by their insolubility in the solvent system of the reaction in which they are active. This type of catalyst is popular in industrial level chemistry due to the ease of separation from the product solution and potential recycling.[4] Schartz offers a "modern" definition of these catalysts as possessing multiple types of catalytic environments.[5] Metal-particle catalysts are classic examples of compounds that fit this definition. The metal clusters exist in various sizes and form a variety of coordination arrangements with reagents and media in the reaction. The various conditions of the metal particles make full characterization of the catalytic environment difficult. The metal clusters are only catalytically active at their periphery since the internal atoms are buried. Therefore, less poison is required to incapacitate the catalysts than if all the metal atoms were capable of being active.

Homogeneous catalysts are defined as being in the same phase as the reaction or by having only one type of active site.[5] Industry has been slow to integrate these catalysts

since they require more effort to separate from a reaction mixture than their hetero-counterparts.[1] Homogeneous catalysts offer the advantages of being stereotypically more selective, more active, and not as easily poisoned. Also they are fully characterizable by current spectrometric methods, allowing for easier fine-tuning. These advantages have inspired more interest in homogeneous catalysts and have led to the development of such separation technologies as ultra- and nano-filtration, which make these catalytic methods more industrially viable.[4,6]

Enzymatic catalysts are naturally occurring, biologically active proteins. They are notorious for their complex formations with substrates, large degrees of rate acceleration, and high substrate selectivity. Enzymes are rarely used in industry due to their high substrate selectivity, incompatibility with organic solvents, ineffectiveness in abiotic reactions, and sensitivity to temperature and pH. Work has been done to create synthetic enzymes or "synzymes" that could overcome some of the limitations of natural enzymes.[7-11] For example, Suh and coworkers created artificial proteases and nucleases using polymeric scaffolding to imitate the flexible nature of the enzymatic polypeptide backbone.[7] Polymers are logical choices for a cheap, organic soluble, flexible macromolecular support. Polymers are, however, difficult to synthesize discrete size increments and in terms of specific, reproducible placement of the catalytic units. Dendrimers offer an alternative to linear polymers with the advantages of being highly characterizable and easily varied in terms of size.

Dendrimers

Dendrimers are macromolecules consisting of a central core and emanating branch units called dendrons. The various sizes of dendrimers are referred to as generations. Generally higher generations have more branches, though no ubiquitous designation currently exists for acknowledging the number of dendrons present in all dendrimers. Tomalia et al and Newkome et al concurrently developed dendrimer technology in the mid 1980s based on the seminal efforts of Vogtle.[12]

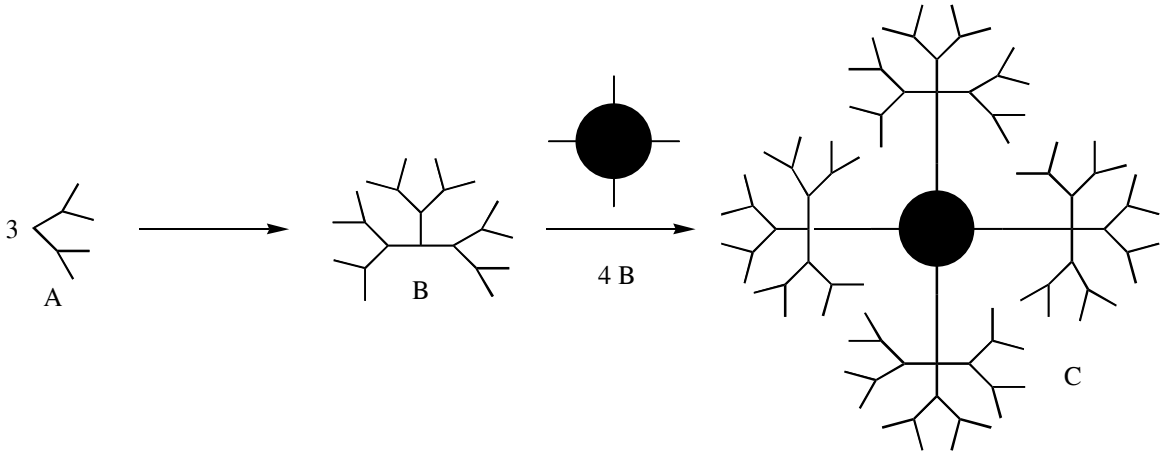

Figure 1.1 Schematic representation of convergent dendrimer synthesis

The two fundamental strategies for dendrimers synthesis are convergent[13] and divergent[14]. Convergent syntheses are initiated by creating the dendrons and then attaching the branches to a core. Divergent syntheses begin with the core and the branches are attached. Higher generations are achieved by repeating the branching process. Convergent methods usually require more complicated chemistry, but offer a more homogenous product. Divergent assembly with its simple, iterative steps is the methodology employed in industry even though the higher generation dendrimers contain

progressively more imperfections. The polypropylene imine denrimer (PPI) is a highly studied, commercially available dendrimer.

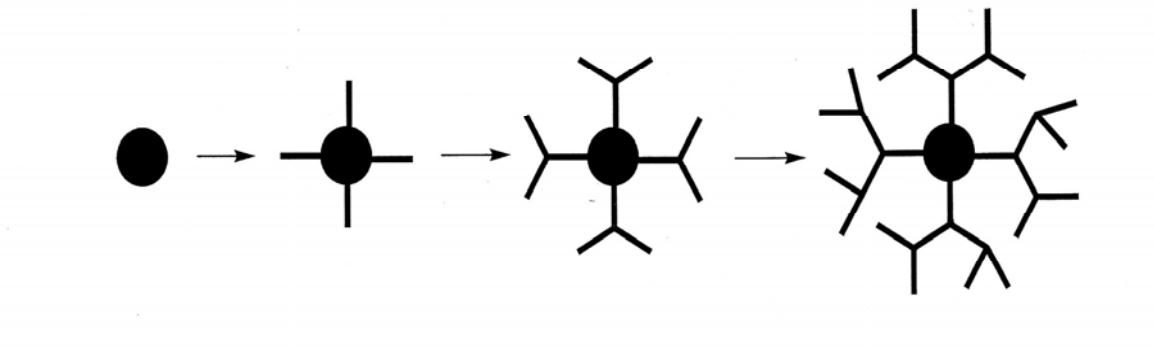

Figure 1.2 Schematic representation of divergent dendrimer synthesis.

PPI dendrimers were initially conceptualized by Vogtle[15] and the synthesis was then refined to an industrially viable process by de Brabander-van den Berg and Meijer.[16,17] PPI dendrimers consist of a diaminobutane core and tertiary amine linkages between carbon spacers terminating in primary amines. The PPI dendrimer synthesis begins with the Michael addition of diaminobutane to four equivalents of acrylonitrile (Scheme 1.1). The resulting cyano functionalities are reduced with Rainey cobalt and hydrogen to primary amines yielding the first generation (G1) PPI dendrimer.

The G1 PPI dendrimers can then be reacted with 8 equivalents of acrylontrile followed by the aforementioned reduction to produce the second generation (G2) PPI dendrimer with 8 terminal primary amines. Iteration of the reactions in the PPI synthesis produces the next generation dendrimer and theoretically doubles the number of terminal primary amine endgroups. Figure 1.3 displays a generation 3 PPI dendrimer. As higher generations are produced, the possibility of side reaction and incomplete reaction

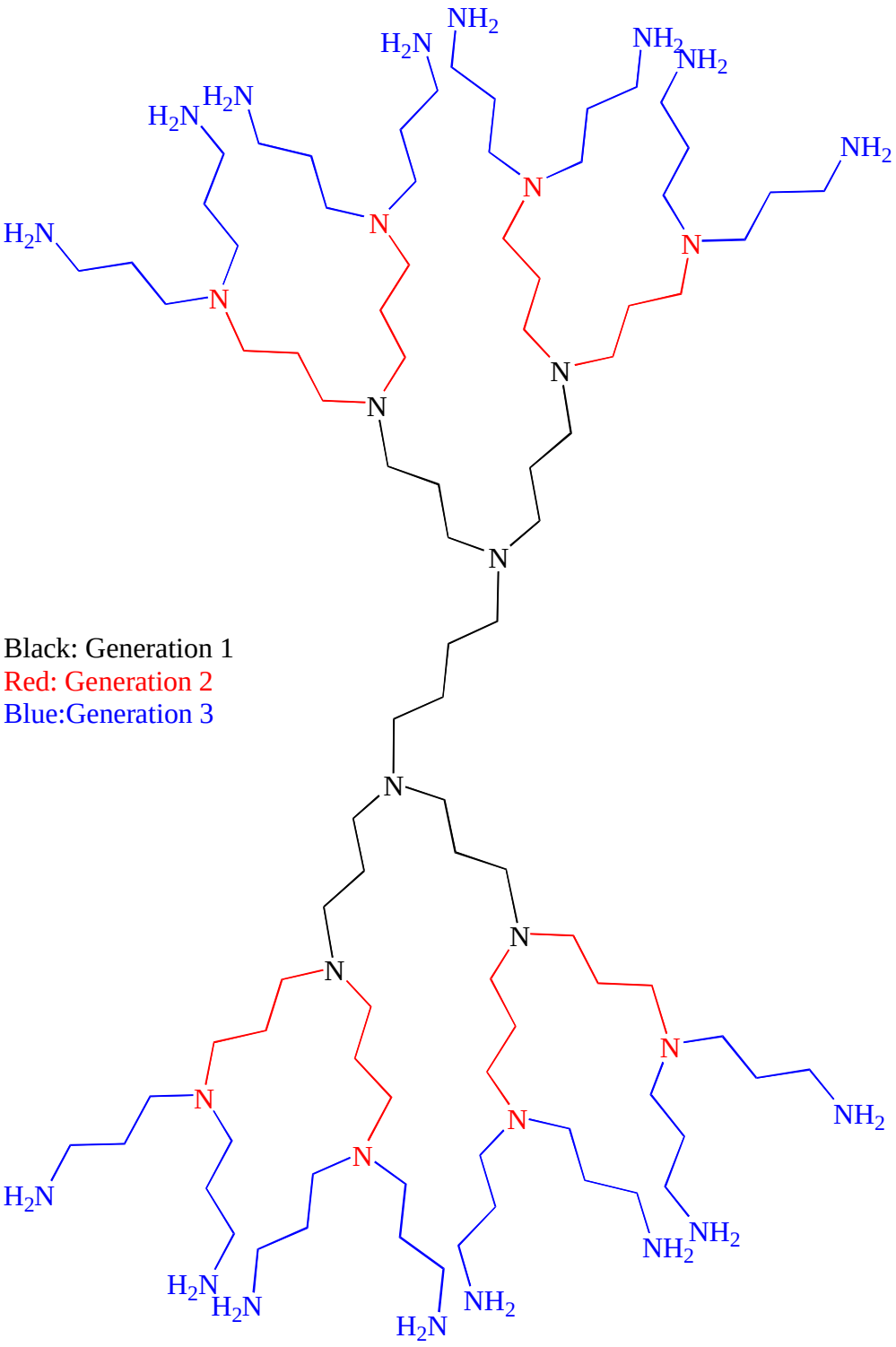

Figure 1.3 Generation 3 PPI dendrimer.

increases. Common flaws in the dendrimer synthesis are incomplete cyanoethylations, retro Micheal additions of cyano alkene and branch cyclizations.[14] The impact of potential dendrimer defects will be discussed in "MALDI Characterization" in Chapter 2.

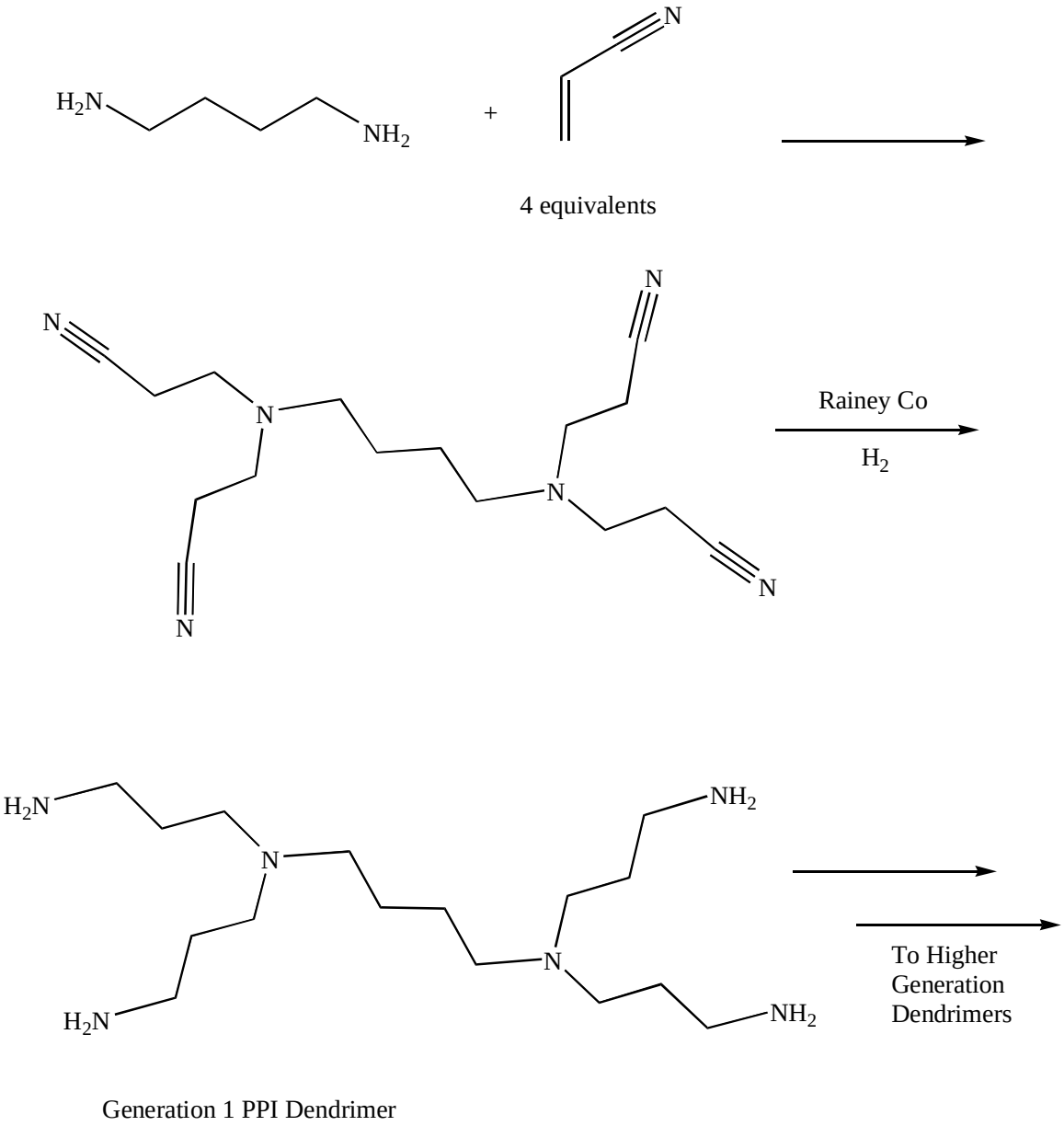

Generation 1 PPI Dendrimer

Scheme 1.1 Synthesis of Generation 1 PPI dendrimer.

Dendrimers are currently popular in catalysis with several reviews written on the subject in recent years.[18-23] Catalytic units can be attached to the interior of the dendrimer framework or around the periphery. Interior dendrimer catalyst are often designed such that the branching subunits create a favorable polar environment to stabilize the transition state of the catalyzed reaction.[22] Steric congestion as substrates pass through the periphery of the dendrimer and the dendritic arms to reach the internal catalytic site tends to slow catalysis and make for slow substrate-catalyst turnover. Periphery functionalized dendrimers offer less steric interference and statistically higher turnover rates. However, stabilization of the transition state of the substrate is dependent on the solvent or a neighboring catalytic unit.[23]

Attaching a catalyst to a dendritic framework increases the size of the catalyst and makes for simpler separation from the product.[21] Most studies show a decrease in the activity of a catalytic unit attached to a dendrimer compared to the free monomer. A few recent studies show enhanced activity of catalytic monomers after attachment to a dendrimer. Frechet and coworkers recently published the first review of dendrimer enhanced catalysts where the catalytic monomers once attached to the dendrimer begin to cooperate to effect greater activity than a solution of the same concentration of unbound monomers.[24] There are still relatively few dendrimer enhanced systems compared to the number of dendrimer repressed systems. The focus of this project is to explore another dendrimer enhanced catalytic system.

Project Background

Suh and coworkers reported attaching three salicylic acid residues, in various proximities to each other, to a linear PPI polymer backbone.[25] The rate of hydrolysis of the peptide backbone of the protein immunoglobulin G (IgG) was measured in the presence of the salicylic acid functionalized polymer. The protein was degraded faster when the acid residues were physically closer to one another. Suh proposed a mechanism that explains the difference in degradation rates by hypothesizing that 2 salicylic acid residues are necessary to cleave the amide bonds of the peptide backbone.[7] Salicylic acid residues attached to a PPI dendrimer should degrade IgG in a fashion similar to the PPI polymer catalyst. The terminal amines of different generations are in different proximities to one another and would afford catalytic units at different proximities if functionalized. Generation 1 through generation 5 salicylic acid (SaI) functionalized PPI dendrimers would theoretically degrade IgG at respectively different rates.

IgG is a commercially available antibody made up of 2 heavy chains (~50 KDa) and 2 light chains (~25 KDa). The molecule is roughly Y-shaped and has a mass of 150 KDa. Figure 1.4 shows a model of IgG. The heavy chains are colored dark gray and the light chains are colored light gray. Given the literature precendent[25] for IgG's peptide cleavage in the presence of a salicylic acid functionalized catalyst, IgG is an excellent choice for this study.

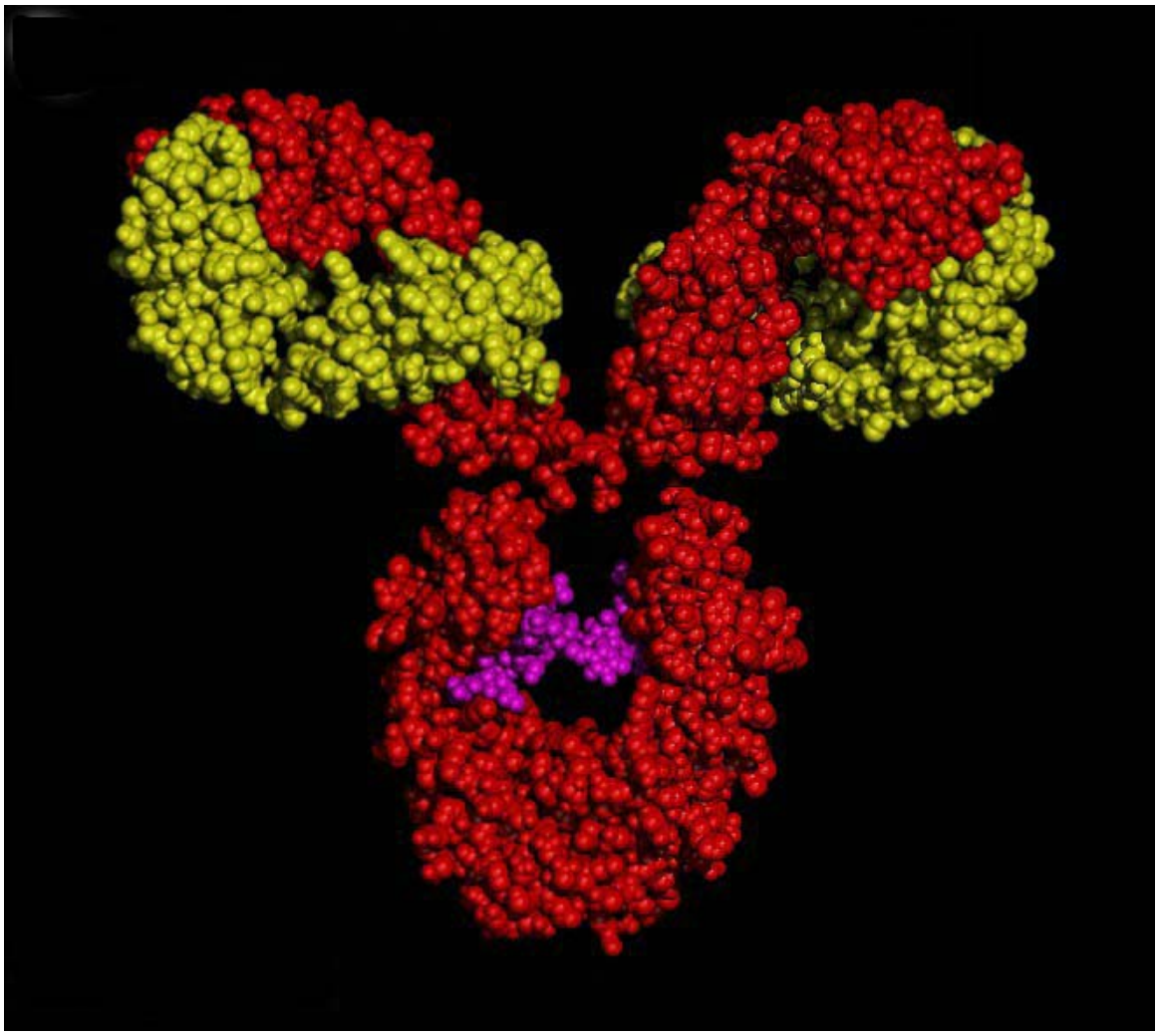

Figure 1.4 Model of the protein Immunoglobulin G.

The synthesis of SaI functionalized dendrimers began with the synthesis of a salicylic acid derivative that could easily be attached to the primary amines coating the exterior of the PPI dendrimers. The Cloninger research group has had great success with thiourea linkages formed by isothiocyanates and the terminal primary amines of polyamidoamine (PAMAM) dendrimers.[26-29] However PAMAM dendrimers contain amide linkages that could be cleaved in a manner comparable to that envisioned for the

IgG amide backbone, hence the PPI dendrimers were chosen as a commercially available, amide free alternative.

Goals and Brief Project Description

The primary goal of this study was to synthesize a dendritic catalyst that displays cooperative function between its peripheral catalytic subunits. A secondary goal was to gain insight into the relative average proximity of the peripheral groups of PPI dendrimers. First, SaI functionalized PPI dendrimers were synthesized using methyl 5-isothiocyanato-2-hydroxybenzoate. The functionalized dendrimers were characterized using ^{1}H NMR, ^{13}C NMR, MALDI-TOF, and Micro-TOF. The dendrimers were then employed in kinetic studies of the rate of IgG hydrolysis. The degradation of IgG was monitored by SDS-PAGE. The rate of dendrimer enhancement was compared between the various generations and against unbound salicylic acid.

Summary of Results

Generation 1-5 SaI functionalized PPI dendrimers were synthesized and characterized. Generation 5 (G5) was the only dendrimer to enhance the cleavage of IgG under the given conditions. G1-G4 and the unbound salicylic acid displayed no detectable activity.

Organization

In Chapter 2, the synthesis of G1-G5 SaI functionalized dendrimers will be discussed followed by characterization techniques and methods. In Chapter 3, the kinetic studies of IgG cleavage of each individual SaI functionalized PPI and unbound SaI will be reported.

CHAPTER TWO

SYNTHESIS OF SALICYLIC ACID FUNCTIONALIZED DENDRIMERS

Background

In this chapter the synthesis and characterization of salicylic acid functionalized PPI dendrimers is described. The kinetic studies to explore rates of cleavage of the peptide backbone of immunoglobulin G (IgG) by the functionalized dendrimers is presented in Chapter 3. Suh and Hah found that a PPI polymer with three salicylic acid residues tethered in close proximity to one another showed enhanced cleavage of IgG when compared to the same polymer with the 3 residues at greater distances from one another.[25]

Comparable cooperativity by the catalytic residues should be observed with the use of a dendrimer as the scaffolding. By covering the periphery of PPI dendrimers with salicylic acid, a rate enhancement should result, given the number of terminal amines that can be used as tethering sites and the flexibility of the branches. The proximity of the residues to one another will be varied by utilizing first through fifth generations of dendrimer.

Synthesis of Methyl 2-Hydroxy-5-isothiocyanatobenzoate

The synthesis of salicylic acid functionalized dendrimers began with the synthesis of a salicylic acid derivative that could easily be attached to the primary amines coating

the exterior of the PPI dendrimers. The salicylic acid derivative target was methyl 2-hydroxy-5-isothiocyanate (**4**).

As shown in Scheme 2.1, 5-nitrosalicylic acid (**1**) was mixed with methanol in the presence of sulfuric acid for 24 hours at reflux. The resulting white powder was washed with cold water and dried under vacuum with phosphorus pentoxide overnight. The product **2** had the distinct smell of artificial cherry flavoring. The characterization data matches that of previous work.[30]

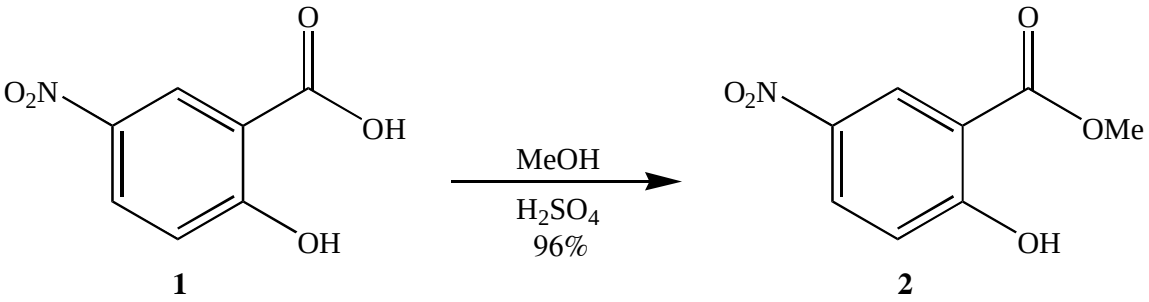

1 **2**

Scheme 2.1 Synthesis of methyl ester **2**.

The nitro group of the methyl ester **2** was reduced to the amine **3** . The palladium was removed by filtering and the solvent was removed under vacuum to afford a brown solid **3** as shown in Scheme 2.2. The melting point of the product recrystalized from water matches previous work.[31]

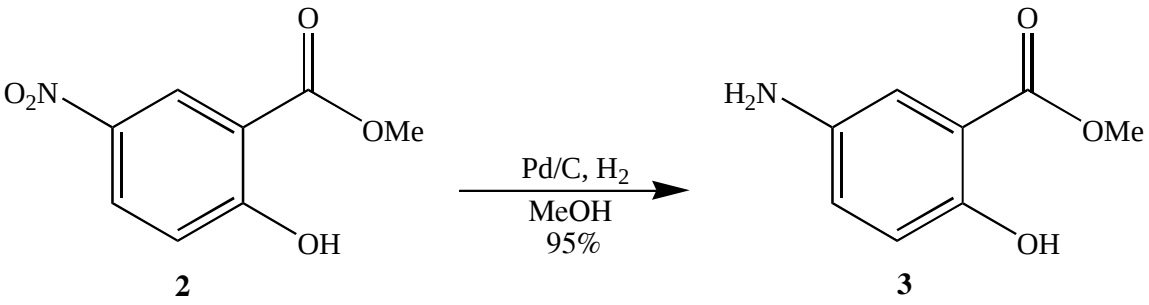

2 **3**

Scheme 2.2 Synthesis of amine **3**.

The amine was converted to an isothiocyanate group by reaction with thiophosgene. Specifically, amine **3** was dissolved in chloroform and added via an addition funnel to a stirring mixture of thiophosgene and water (Scheme 2.3). The amine solution was added over an hour. Addition of the amine to the thiophosgene was necessary to keep the amine concentration in the reaction mixture low as possible to avoid dimer formation. After amine addition the biphasic mix was stirred for 6 hrs and the layers were separated. The aqueous layer was washed with chloroform and the organic layer was washed with water. The $CHCl_3$ layers were combined and solvent was removed under vacuum, affording a purple solid. The impure product was filtered over silica to afford the off-white isothiocyanate **4** primed for dendrimer tethering. Having the isothiocyanate at the 5 position is ideal given that Suh and Hah tethered their catalytic subunits at the same aromatic location.[25]

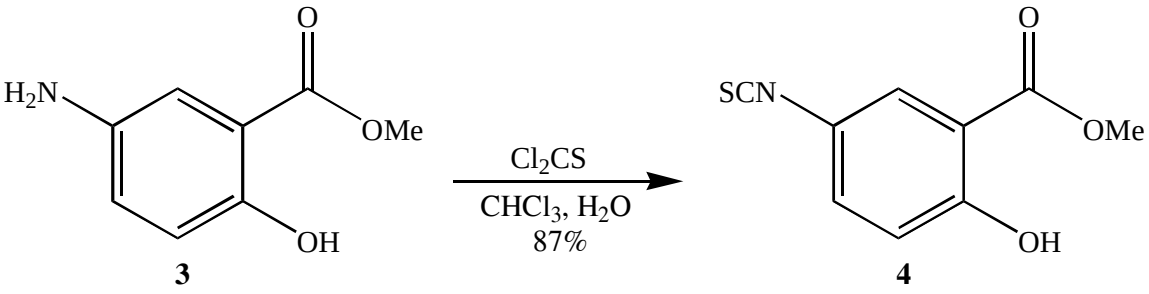

Scheme 2.3 Synthesis of isothiocyanate **4**.

Dendrimer Functionalization and Saponification

PPI dendrimer and **4** were mixed in a scintillation vial with dimethyl sulfoxide (DMSO) and stirred for 1 h (Scheme 2.4). The solution was dialyzed against 9:1 DMSO

and water and then lyophilized. The products were characterized by NMR and MALDI-TOF. The characterization data will be discussed at length later in this chapter.

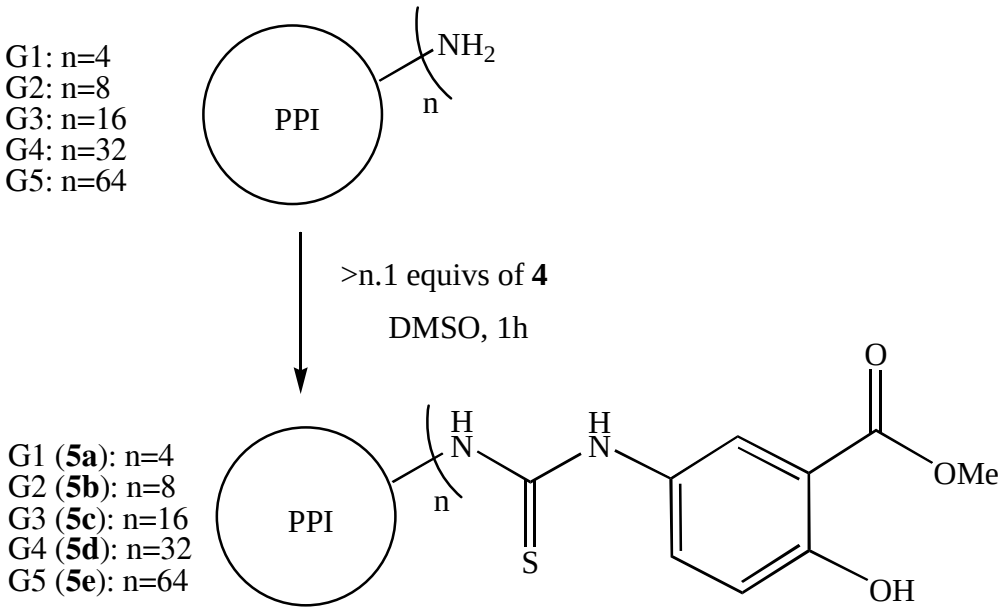

Scheme 2.4 Synthesis of methyl salicylate functionalized PPI using **4**.

The methyl ester functionalized dendrimers **5** were dissolved in DMSO in a scintillation vial. A solution of lithium hydroxide in deuterium oxide was added (Scheme 2.5) and the vials were set in an oven at 51 °C for 6 hours. The solution turned from yellow to a dark green. Deuterium oxide was used instead of water to avoid contamination by Fe^{+3} ions. Three salicylic acid residues will bind Fe^{+3} tightly[32] thereby poisoning the catalytic activity. The solution was neutralized to ~pH 7.6 with hydrochloric acid (HCl) in D_2O. The resulting mix was lyophilized and reconstituted in a minimal amount of DMSO. The concentration of the solution was determined by variations on a no-D NMR technique[33,34] and the products were used in the protein degradation studies without further purification.

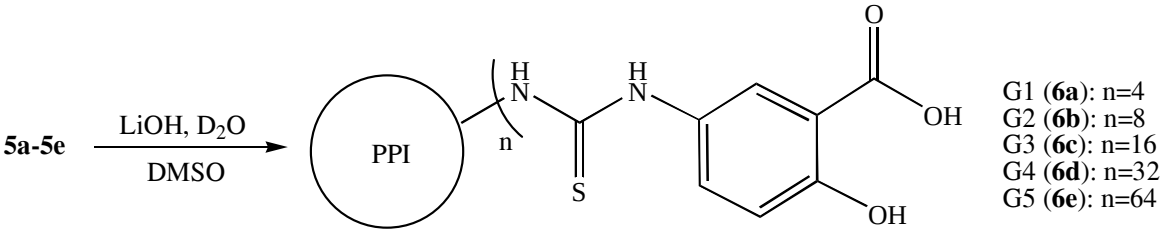

Scheme 2.5 Saponification of methyl salicylate functionalized PPI

NMR Characterization

The ^{1}H NMR spectrum of the ester functionalized dendrimer **5b** is shown in Figure 2.1 and the spectrum of **6b** is shown in Figure 2.2. A general procedure for ^{1}H NMR sample preparation is included in the experimental section of this chapter. The methyl ester proton resonance at 3.9 ppm in **5b** is not present in **6b**. The resonanace at 4.1 ppm in **6b** is a solvent peak. The methyl ester peak shifted to 3.6 ppm and the degradation of the peak was observed over time by ^{1}H NMR (data not shown). Figure 2.3 shows the ^{1}H NMR spectra of **5e.** Figure 2.4 shows the ^{1}H NMR spectra of **6e**. In the larger generation dendrimers, the loss of resolution of the splitting in the aromatic proton resonances and the general broadening of all the peaks are due to the much slower tumbling of the larger scaffolding. Again, the methyl ester proton resonance is absent in **6e**. The thiourea proton resonances and the phenol proton resonance are not visible in Figure 2.2 and 2.4. The ^{1}H NMR spectra of the acid functionalized denrimers were taken in a mixture of d_6-DMSO, D_2O, and LiOH. Deuterium exchange explains the lack of thiourea proton resonances and the phenol proton resonance in Fig. 2.2 and 2.4. By conducting saponification of compounds **5a-5e** with deuterated solvents, integration of

the interior dendrimer proton resonances that would otherwise be buried under solvent peaks was obtainable. Solvent penetration of the interior of the dendrimer has been reported.[35] and experienced within the Cloninger group. Attempts to remove all solvent from the acid functionalized dendrimer resulted in an insoluble product, a phenomenon that has been observed repeatedly within the Cloninger research group.

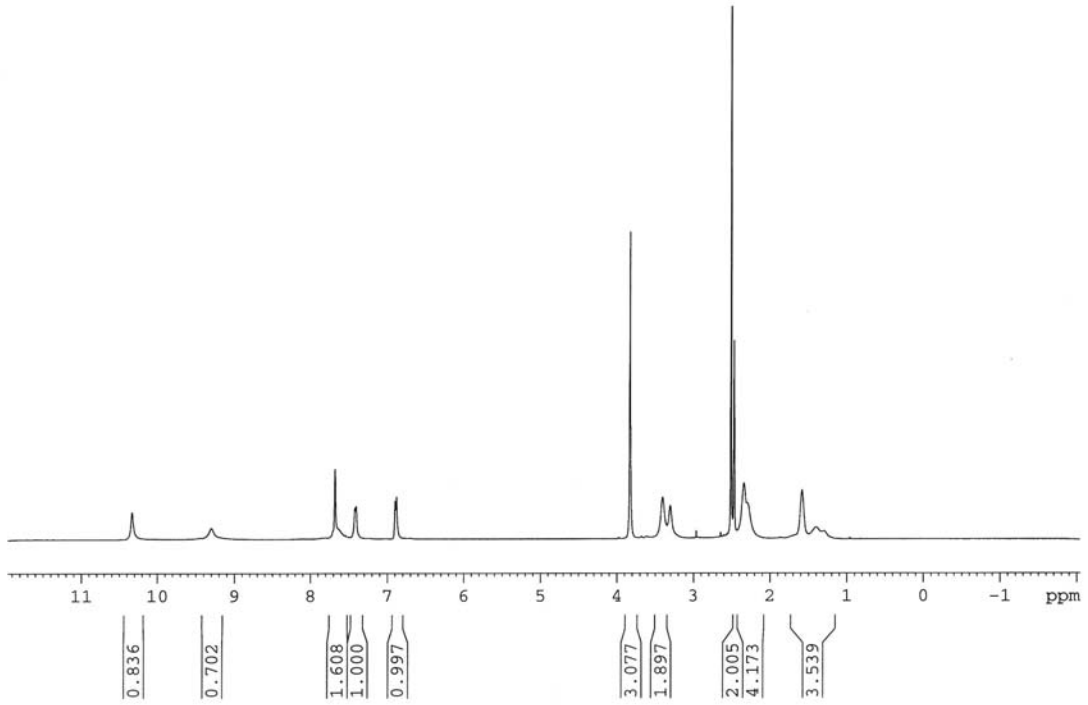

Figure 2.1 ^{1}H NMR spectrum of **5b** in d_6-DMSO.

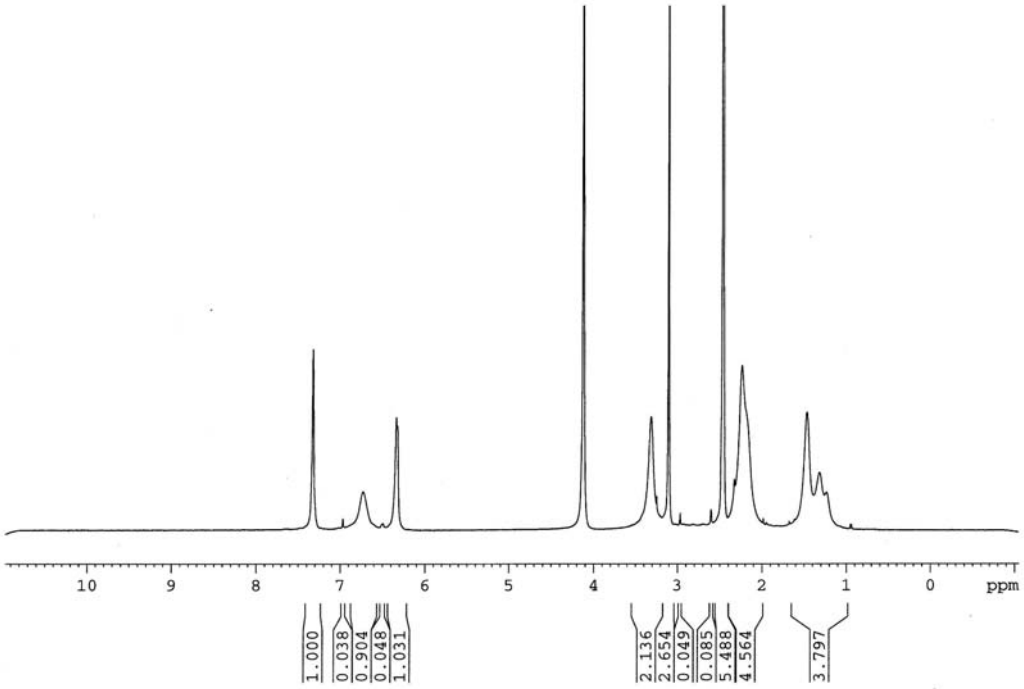

Figure 2.3 ^{1}H NMR spectrum of **6b** in d_6-DMSO/D_2O.

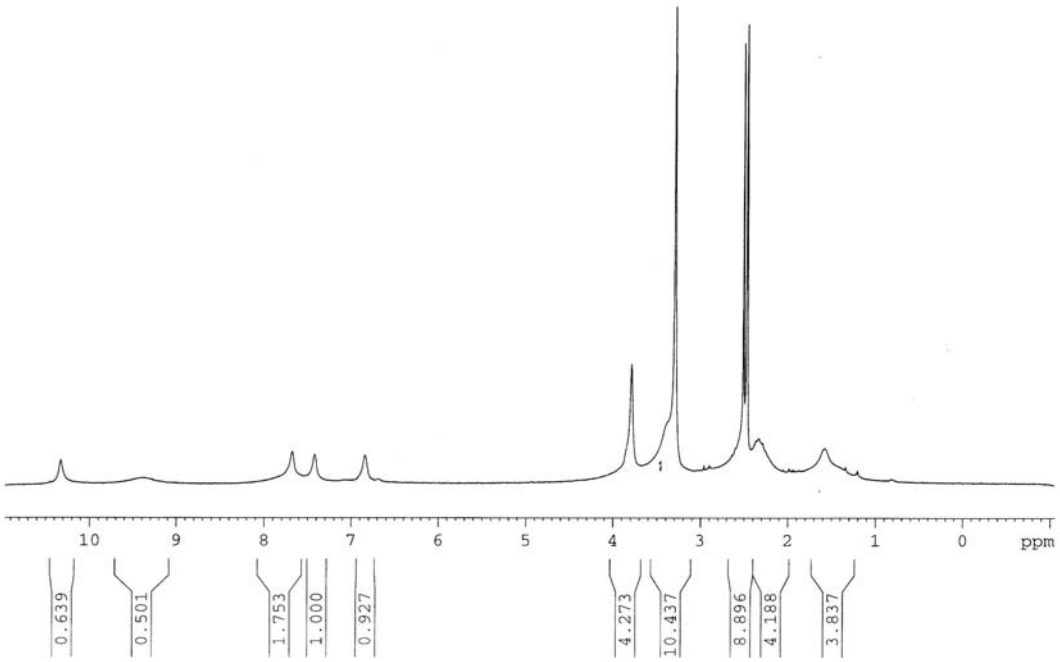

Figure 2.3 ^{1}H NMR spectrum of **5e** in d_6-DMSO.

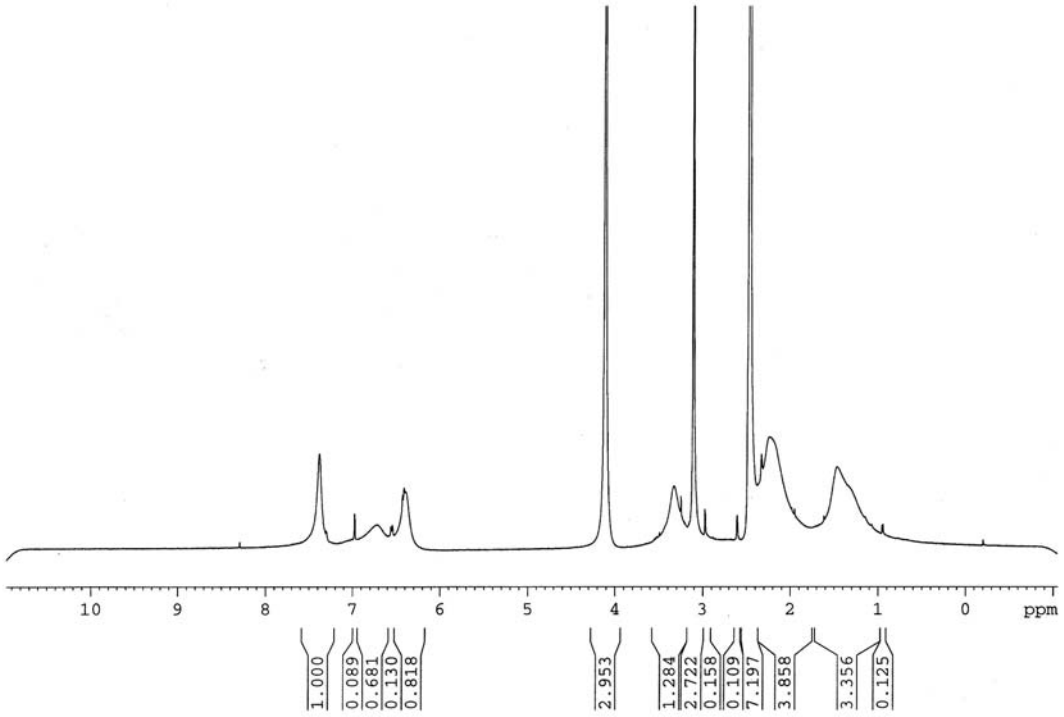

Figure 2.4 ^{1}H NMR spectrum of **6e** in d_6-DMSO/D_2O.

MALDI-TOF Characterization

Matrix-assisted laser desorption ionization time of flight (MALDI-TOF) mass spectrometry has been a staple characterization technique for dendrimers in the Cloninger labs. MALDI-TOF's defining characteristic is the use of a matrix to aid in the ionization of an analyte. Macromolecules (i.e. dendrimers) would fragement if directly ionized by a laser given the relatively high amount of energy necessary. The matrix absorbs the energy from the laser and then diffuses it into the analyte creating a "soft" ionization method.[36] Figures 2.5, 2.6, 2.7, 2.8, and 2.9 show the MALDI-TOF spectra of **5a-5e** respectively. A general procedure for the MALDI-TOF analysis of **5a-5e** is included in the experimental section of this chapter.

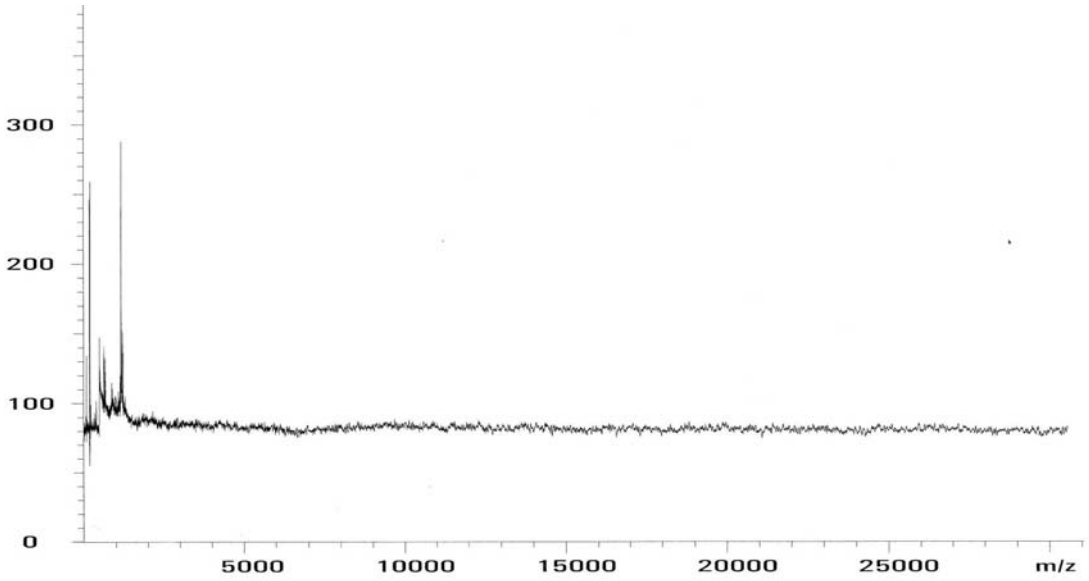

Figure 2.5 MALDI spectrum of **5a.** (M_w=1153)

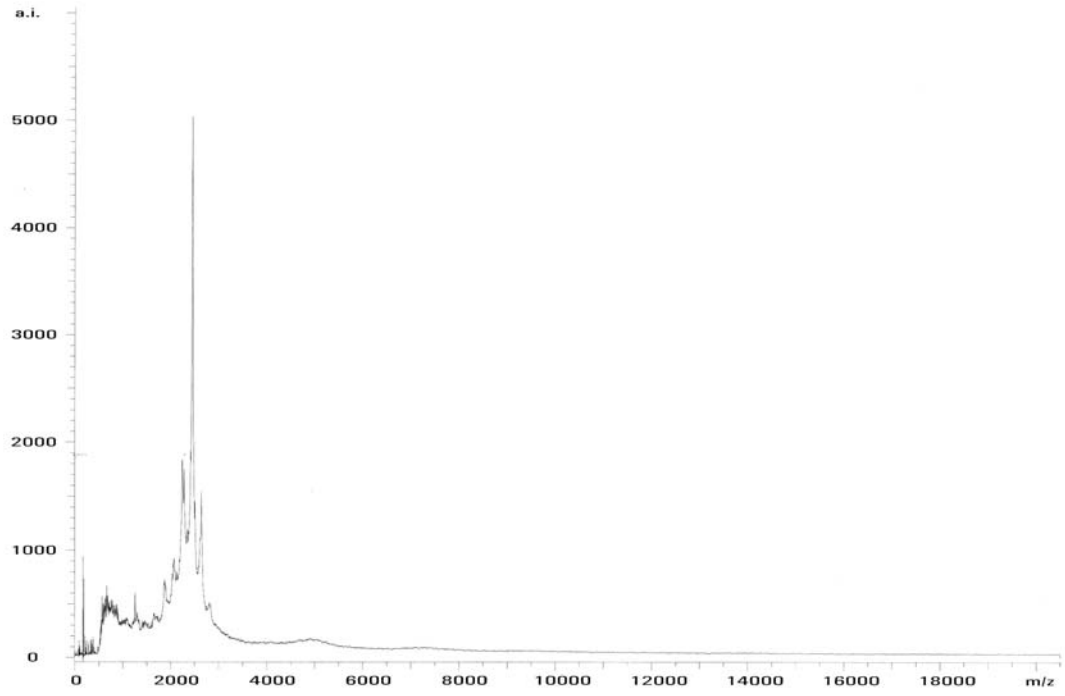

Figure 2.6 MALDI spectrum of **5b.** (M_w=2446)

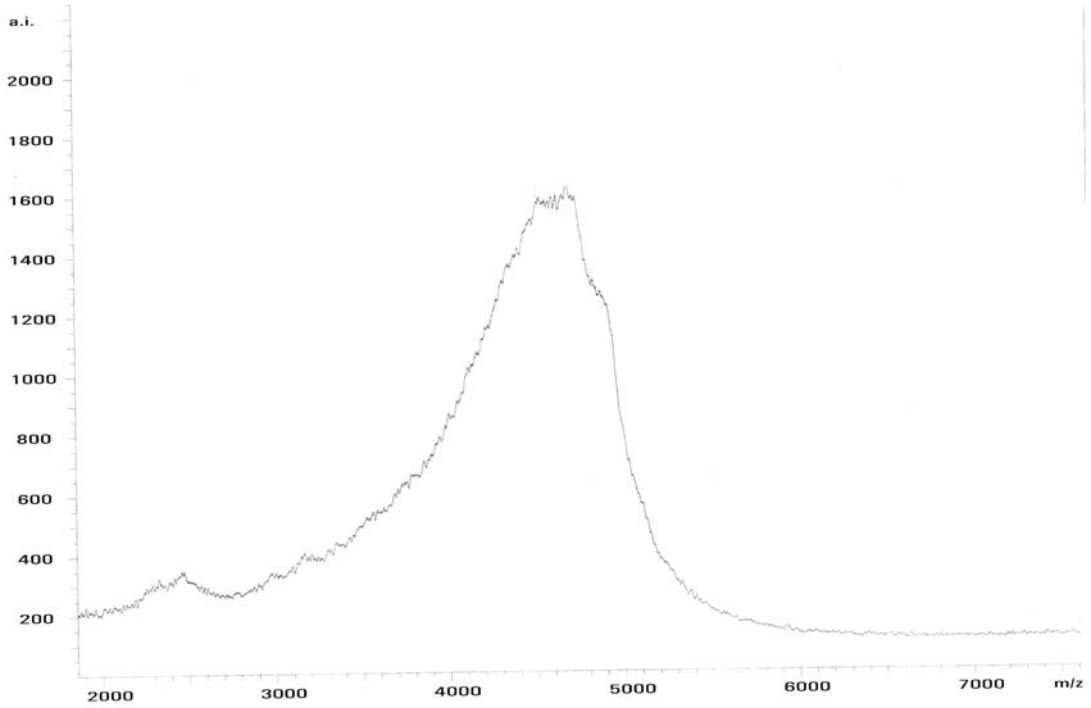

Figure 2.7 MALDI spectrum of **5c.** (M_w=4200)

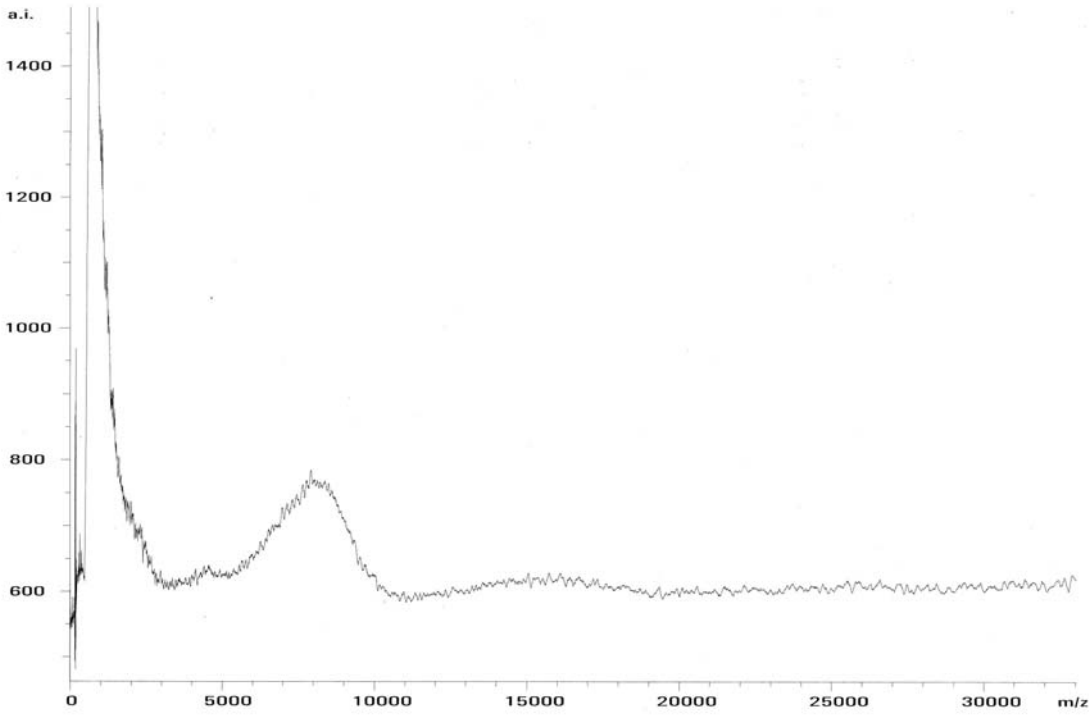

Figure 2.8 MALDI spectrum of **5d.** (M_w=9200)

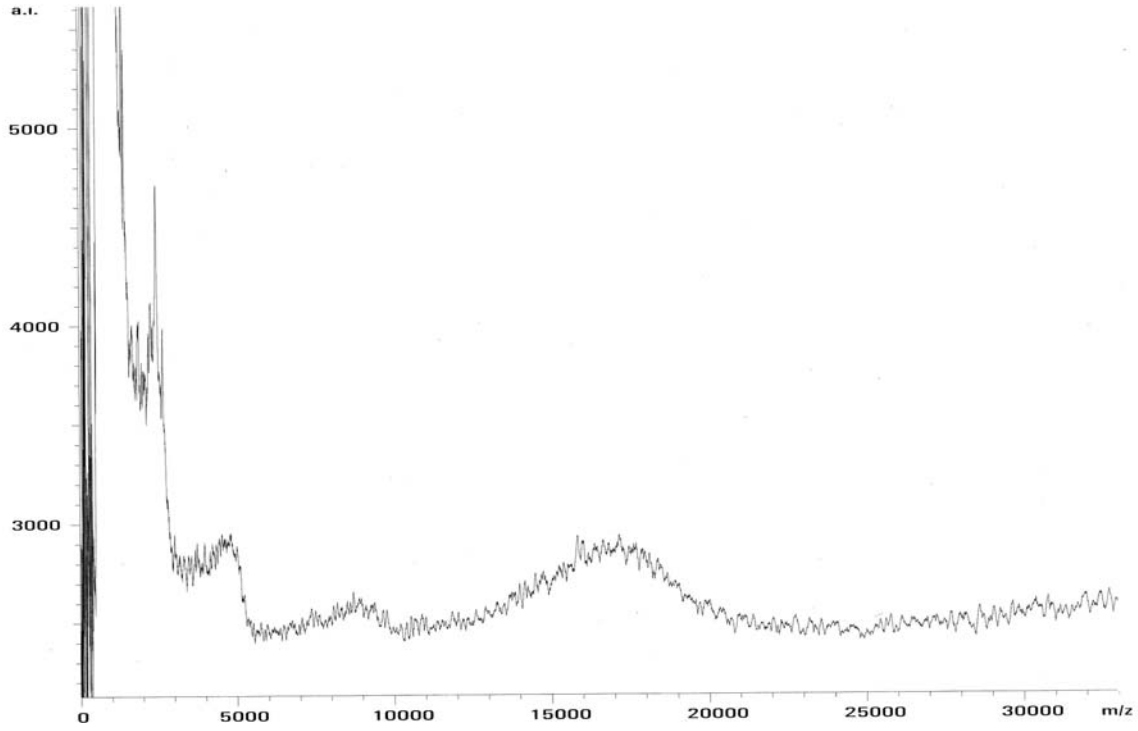

Figure 2.9 MALDI spectrum of **5e.** (M_w=16600)

As the generation of the dendrimer increases, so does the width of the peak. The peak widening is indicative of the divergent synthesis scheme of the PPI dendrimer. The chances of imperfections in the dendrimer increase as the iteration of the synthesis steps is repeated. The weight average molecular weights (M_W) were found using the XTOF version 5.1.1 software on a Bruker Biflex III instrument. The average number of salicylic acid residues **4** attached to the dendrimer was determined by subtracting the mass of the unfunctionalized PPI from the M_W determined by the MALDI-TOF spectrum. The difference was divided by the molecular weight of **4** affording in the average number of methyl salicylates bound to the dendrimer. The M_W's for **5c-5e** are lower than the theoretical molecular weights (Table 2.1) suggesting that the dendrimers are imperfect, all terminal amines are not reacting with **4**, or the analyte is fragmenting during ionization.

Given the MALDI-TOF spectra of the unfunctionalized PPI dendrimers (Figure 2.10, 2.11, 2.12, 2.13), it is clear that G1-G3 are dominantly homogeneous while G4 and G5 are more heterogeneous, but not grossly imperfect. The mass spectroscopy data for **6a-6e** was analyzed to determine whether **5c-5e** are being fragmented by ionization or the crowding of the attached salicylates is preventing all the terminal amines from being bound as the thiourea.

Table 2.1 MALDI and Micro-TOF data for **5a-5e** and **6a-6e**.

Generation	Theoretical # of amines (M_W)	# of SaI Exp. (M_W)[a] **5a-5e**	# of SaI Exp. (M_W)[a] **6a-6e**	% loading **5a-5e** (**6a-6e**)
G1	4 (316)	4 (1153)	4 (1087)[b]	100 (100)
G2	8 (773)	8 (2446)	8 (2312)[b]	100 (100)
G3	16 (1656)	12 (4200)	16 (4795)[b]	75 (100)
G4	32 (3514)	27 (9200)	30 (9352)	84 (94)
G5	64 (7168)	45 (16600)	43 (15548)	70 (67)

[a] M_W determined by MALDI
[b] M_W determined by Micro-TOF

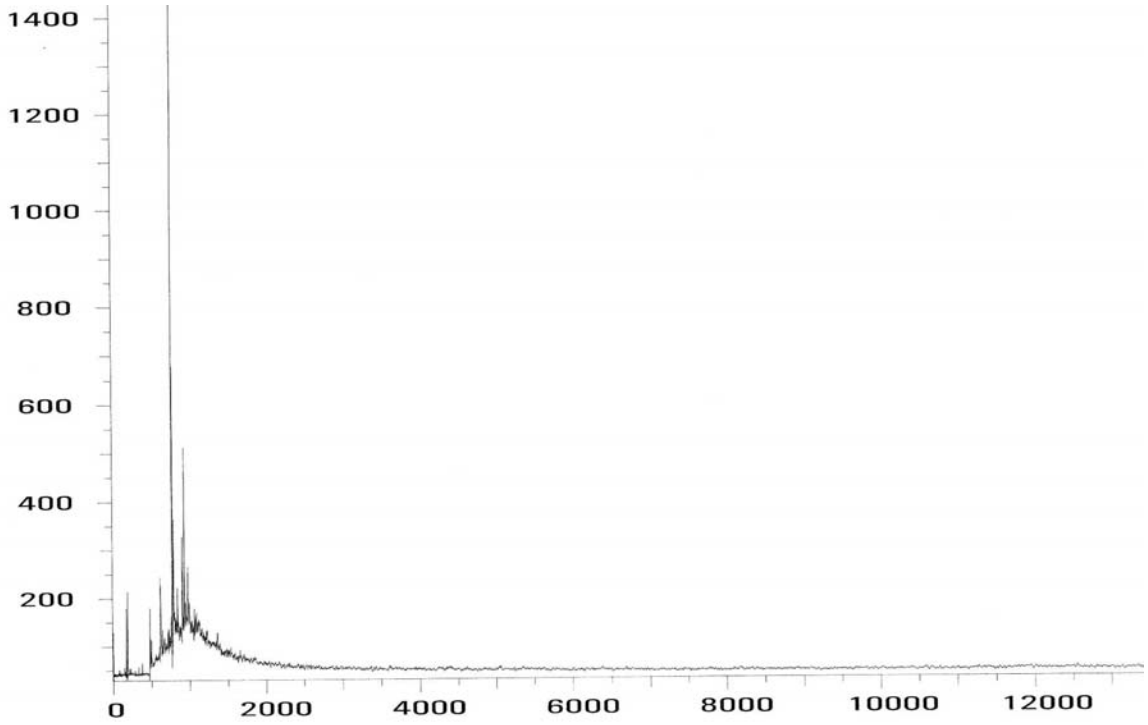

Figure 2.10 MALDI spectrum of generation 2 PPI dendrimer.

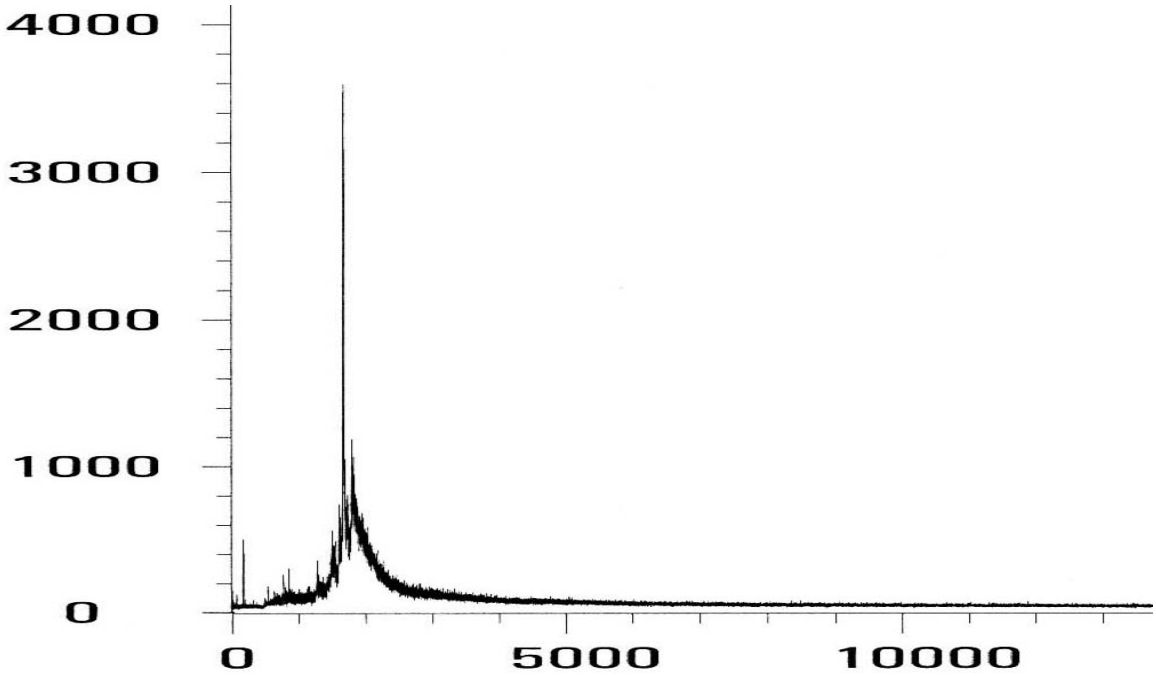

Figure 2.11 MALDI spectrum of generation 3 PPI dendrimer.

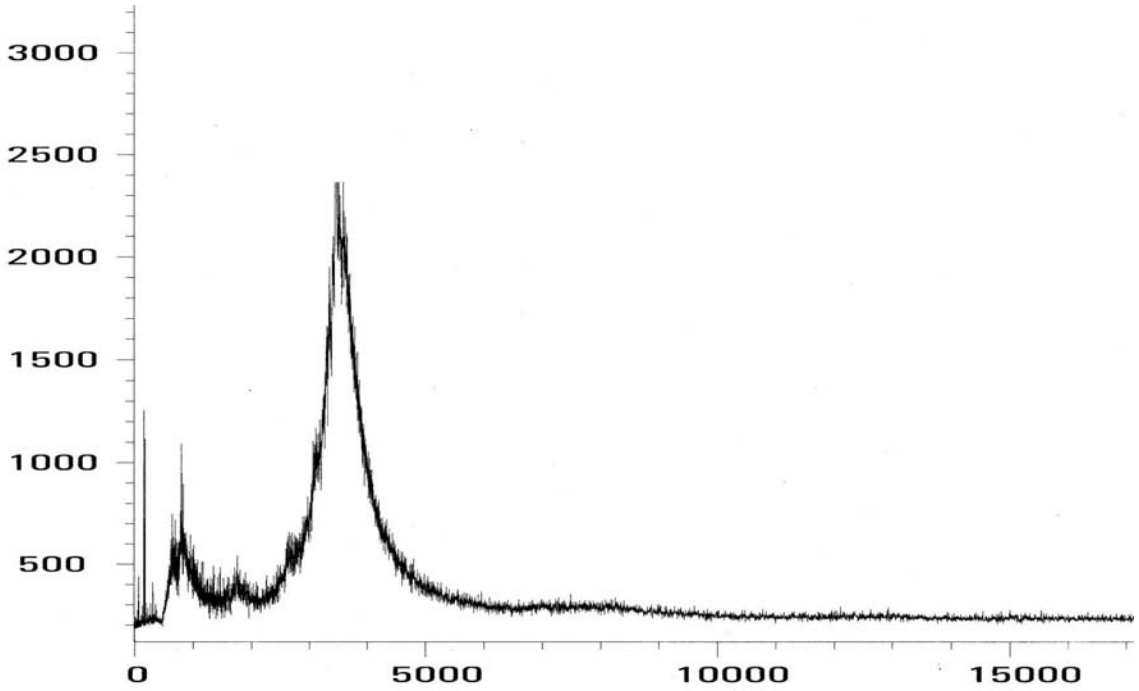

Figure 2.12 MALDI spectrum of generation 4 PPI dendrimer.

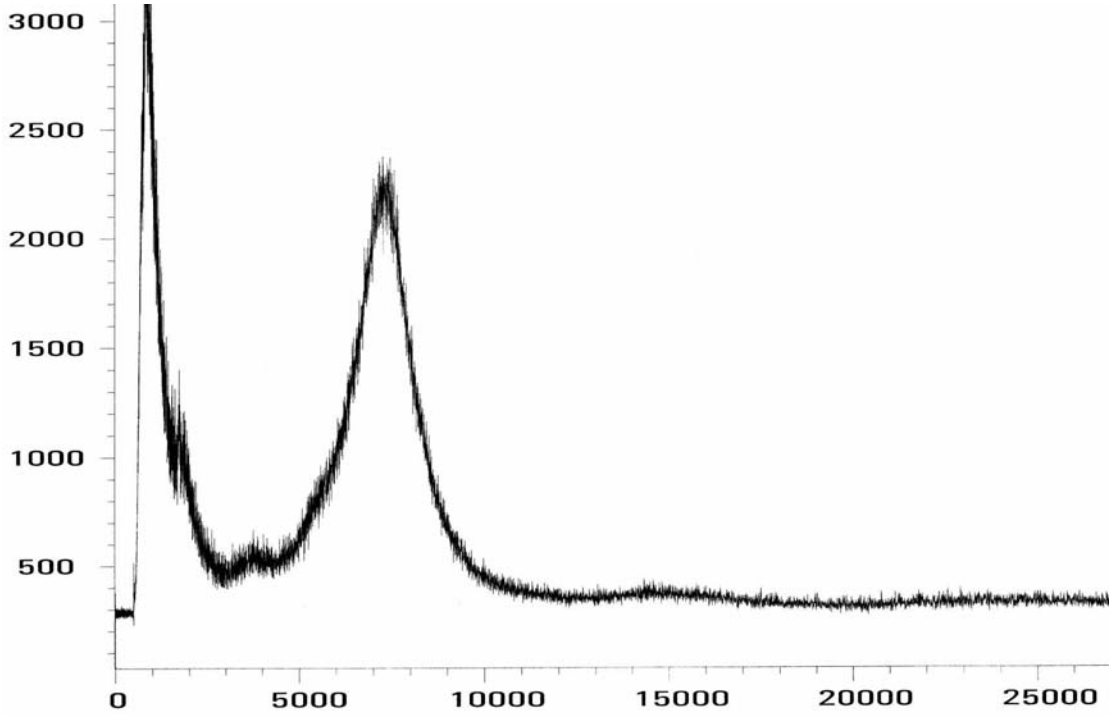

Figure 2.13 MALDI spectrum of generation 5 PPI dendrimer.

Figure 2.14, 2.15, and 2.16 shows the MALDI-TOF spectra for **6c**-**6e** respectively. The spectra of **6c**-**6e** were acquired in negative ion mode. Compounds **6a**-**6e** are soluble at high pH and are marginally soluble in DMSO and DMF at room temperature. The MALDI-TOF samples for **6a**-**6e** were prepared in the same fashion as **5a**-**5e**, except that the solutions of the matrix indolacrylic acid (IAA) were 5% aqueous ammonia hydroxide rather than DMF. A general procedure for the MALDI-TOF analysis of **6a**-**6e** is included in the experimental protocols for this chapter. The spectra of **6a**-**6e** have a large matrix peak. The spectra for **6a** and **6b** were impossible to acquire under these conditions because the molecular weights of the matrix and the dendrimer are similar.

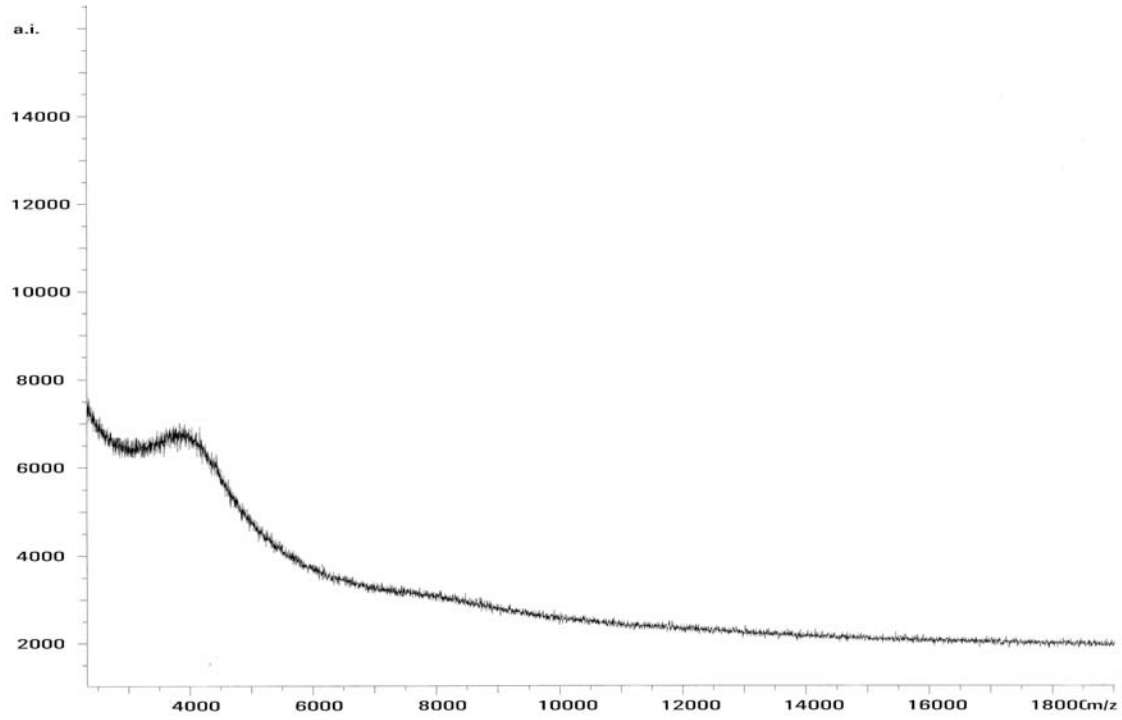

Figure 2.14 MALDI spectrum of **6c.** (M_w=4626)

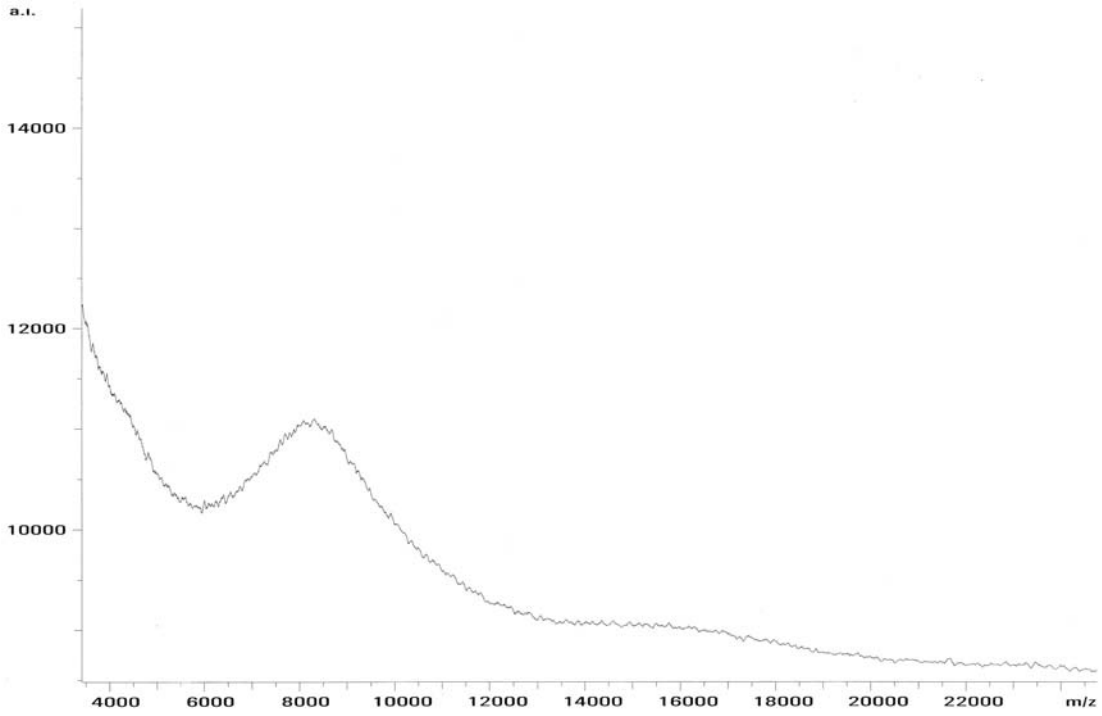

Figure 2.15 MALDI spectrum of **6d.** (M_w=9352)

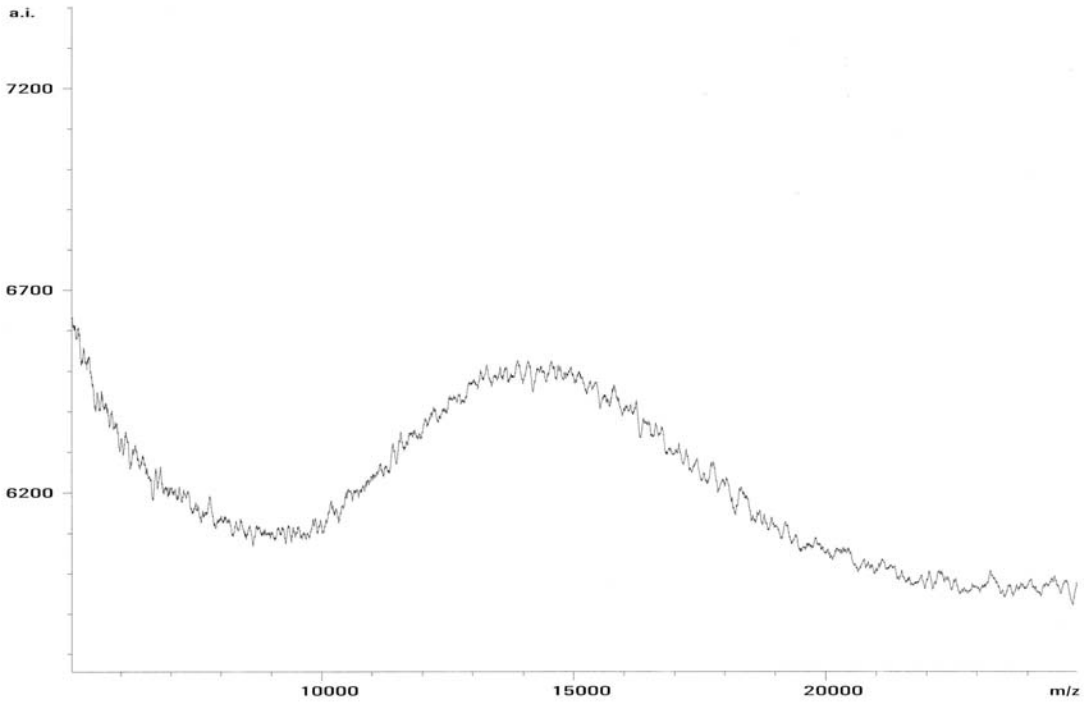

Figure 2.16 MALDI spectrum of **6e.** (M_w=15548)

Brett Wenner of Bruker Daltonics analyzed **6a-6c** by Micro-TOF on a Bruker Micro-TOF instrument. Micro-TOF is an electrospray ionization time of flight mass spectrometry technique. A liquid (analyte and neutral solvent) is forced through a small charged metal capillary tube with a neutral carrier gas. The tube charges the analyte molecules in the liquid. Since like charges repel, the liquid forms an aerosol of small droplets. The carrier gas evaporates the solvent and the analyte ions continue to the mass analyzer. A general procedure for the sample preparation is included in the experimental section of this chapter.

Figure 2.17 shows the micro-TOF spectra of **6a** and Figure 2.18 shows the micro-TOF spectra of **6b**. The spectra show fully functionalized PPI dendrimers in various charged states. Figure 2.19 shows the micro-TOF spectra of **6c**. Figure 2.19 shows a fully functionalized dendrimer peak and two partially functionalized peaks (n=14,15, and 16). Table 2.1 shows the MALDI and Micro-TOF data for **6a-6e.** The micro-TOF spectrum show a much higher average molecular weight than that obtained by the MALDI-TOF spectrum of the same compound in Figure 2.13. The micro-TOF results suggest that the MALDI-TOF conditions are fragmenting **5c-5e** and **6c-6e** upon ionization. Given that MALDI matrices are aromatic compounds, **5a-5e** and **6c-6e** are effectively dendrimer-supported matrix, which explains how conditions necessary to initiate ionization could result in fragmentation. Micro-TOF spectra for **6d** and **6e** were unavailable.

Compounds **6a-6c** must have different average proximities between their respective SaI functional group since all terminal amines were reacted with **4**. However

the difference in the average proximity of the endgroups of **6d** and **6e** is initially unclear. If rate of enhancement is to be varied by generation of PPI, then the proximity of the endgroups must differ from generation to generation.

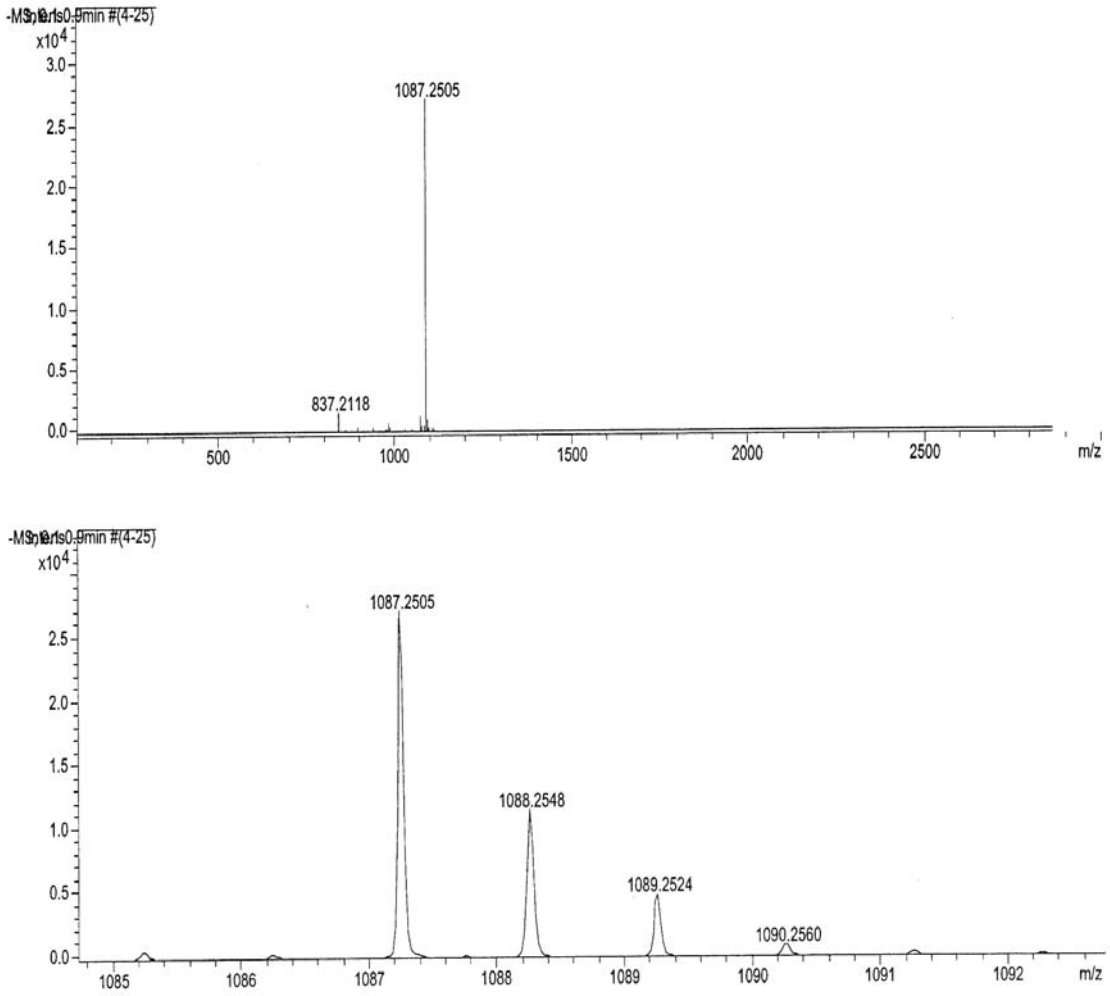

Figure 2.17 Micro-TOF results for **6a**. (M_w=1087)

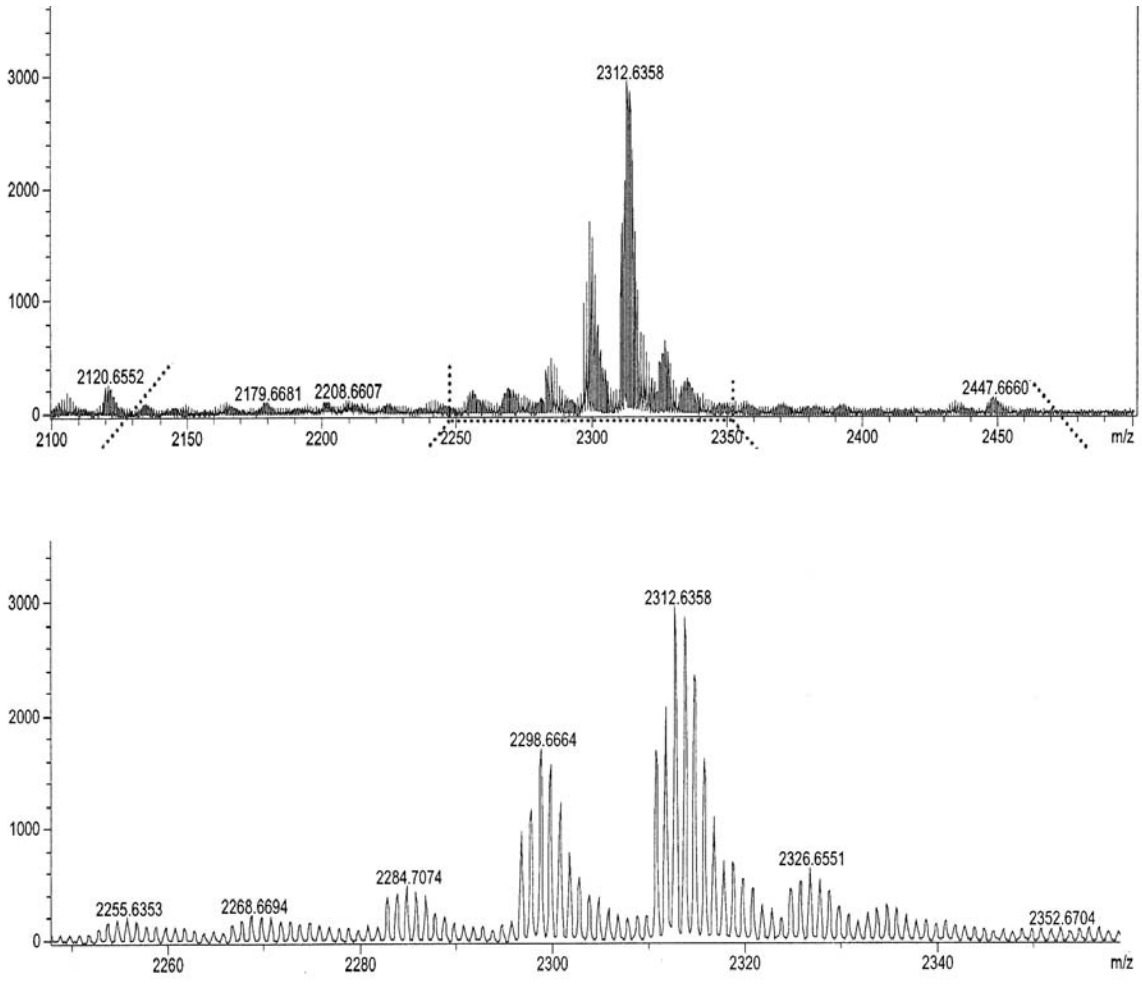

Figure 2.18 Micro-TOF results of **6b**. (M_w=2312)

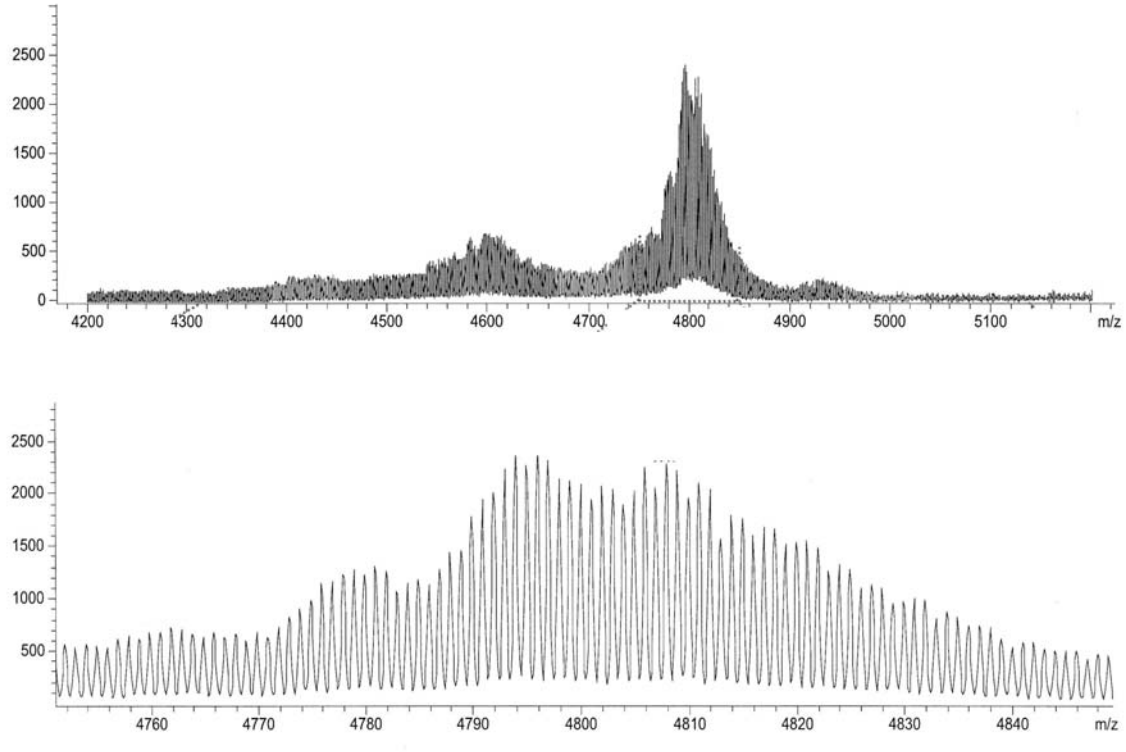

Figure 3.19 Micro-TOF results for **6c**. (M_w=4795)

Functional groups at the periphery of various generations of dendrimer will be in closer proximity to one another as the generation of the dendrimer is increased.[29] Until a point of steric saturation is reached, the functionalization of different generations of dendrimers will result in endgroups with different average proximities to one another. When a point is reached where sterics are preventing some terminal dendrimer sites from being functionalized then the endgroups will be at the same average proximity for all subsequent generations of dendrimer. Compound **6e** showed enhancement of the rate of cleavage of IgG and **6d** did not (see Chapter 3), the SaI units of **6e** are in closer average proximity than the endgroups of **6e**. Therefore the endgroups of **6c** and **6d** must have

different average proximities because the point of steric saturation of loading has not been reached.

Summary

In summary, SaI functionalized PPI dendrimers **6a-6e** have been synthesized using isothiocyanate **4** and characterized using NMR, MALDI-TOF, and Micro=TOF. MALDI data for **6a** and **6b** was not obtainable by the methods employed. Micro-TOF data for **6a** and **6b** correlated with MALDI data for **5a** and **5b**. Micro-TOF data for **6c** did not correlate with MALDI data for **5c** or **6c**. The contradiction showed that the MALDI conditions employed were fragmenting the **5c-5e** and **6c-6e** upon ionization. SaI functionalization of the PPI periphery is more extensive than the employed MALDI techniques are capable of detecting. Given the results of the rate of cleavage studies of IgG it is clear that **6a-6e** respectively possess SaI units in different relative average proximities to one another.

Experimental Procedures

General methods. General reagents were purchased from Acros and Aldrich chemical companies. Solvents and reagents were used as received. Melting points were acquired with a Mel-Temp II instrument after recrystallization and were uncorrected.[30,31] High Resolution Mass Spectrometry was done by Dr. Joe Sears in the Montana State University Mass Spectroscopy facility.

MALDI. Matrix assisted laser desorption ionization (MALDI) mass spectra were acquired using a Bruker Biflex-III time-of-flight mass spectrometer. Spectra of all functionalized dendrimers were obtained using a *trans*-3-indoleacrylic acid (IAA) matrix. Compounds **6c-6e** were analyzed in an 5% ammonia hydroxide and IAA solution in negative ion mode. IAA was recrystallized from absolute ethyl alcohol. Leucine Enkenaphalin (MW 555.6 g/mol) and Trypsinogen (MW 23,982 g/mol) were used as external standards. Standards were purchased from Sigma and used without further purification. A 1 part to 4 parts serial dilution series starting with a 1:200 analyte to matrix ratio and diluted with 100 mM matrix solution was loaded on the MALDI sample plate. The volume of the aliquot loaded on the plate (4-8 μL) depended upon the condition of the plate surface. Positive and negative ion mass spectra were acquired in linear mode and the ions were generated by using a nitrogen laser (337 nm) pulsed at 3 Hz with a pulse width of 3 nanoseconds. Ions were accelerated at 19-20,000 volts and amplified using a discrete dynode multiplier. Spectra (100 to 200) were summed into a LeCroy LSA1000 high-speed signal digitizer. Spectra were optimized by varying laser power on the sample of matrix/analyte mix that yielded the strongest signal. All data processing was performed using Bruker XMass/XTOF V 5.0.2. Molecular mass data and polydispersities of the broad peaks were calculated by using the Polymer Module included in the software package.

Electrospray. Micro-TOF experiments were performed by Brett Wenner of Bruker Daltonics on a Bruker microTOF instrument. Samples were reconstituted in 500

μL of 100 mmol ammonia hydroxide and diluted 10 fold with methanol. The analysis was run in negative ESI mode with direct infusion at 2μL per minute .

NMR. ^{1}H NMR spectra were recorded on Bruker DPX 300 (300 MHz) and Bruker DPX-500 (500 MHz) spectrometers. Chemical shifts are reported in ppm from tetramethylsilane with the residual protic solvent resonance as the internal standard (chloroform: δ 7.24 ppm; methanol δ 4.87, 3.31 ppm; dimethyl sulfoxide: δ 2.50 ppm). Data are reported as follows: chemical shift, multiplicity (s = singlet, bs = broad singlet, d = doublet, dd = doublet of doublets, bd = broad doublet, m = multiplet, app = apparent), integration, coupling constants (in Hz) and assignments. ^{13}C NMR spectra were recorded on a Bruker DPX 500 (125 MHz) spectrometer with complete proton decoupling. Chemical shifts are reported in ppm from tetramethylsilane with the solvent as the internal standard ($CDCl_3$: δ 77.0 ppm; methanol δ 49.15 ppm; dimethyl sulfoxide 39.15 ppm)

No-D NMR Variant.[33,34] A known volume of dendrimer **6a-6e** in d-DMSO from a stock solution was mixed with a known volume of DMF. ^{1}H NMR (500 MHz) spectra were recorded with no solvent lock. The magnet was shimmed using the FID. The ratio of the integral of the DMF resonance to one of the aromatic proton resonances is equal to the molar ratio. The known volume of DMF was converted to moles and when multiplied by the mole ratio the amount of moles of SaI was determined. The moles of SaI divided by the known volume of solution used yielded the concentration of SaI in the stock solution.

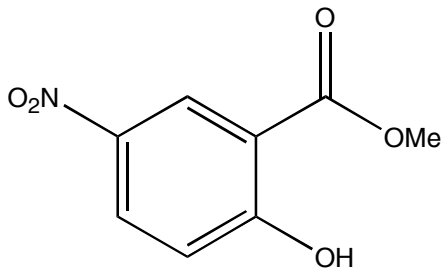

Methyl 2-Hydroxy-5-nitrobenzoate **(2)**. A mixture of 3.37 g (18.4 mmol) **1** in 11 mL of methanol with 1 mL of 97% sulfuric acid was refluxed for 24 h. The white precipitate that formed was washed with 50 mL of cold deionized water and dried with phosphorus pentoxide *in vacuo* to give 3.48 g (17.6 mmol) of an off white powder in 96% yield. A small amount approximately 10 mg was recrystallized from methanol: m.p. 109-110 °C; ^{1}H NMR (300 MHz, $CDCl_3$) 11.4 (s, 1H, O***H***), 8.78 (d, 1H, J = 2.8 Hz, C6-***H***), 8.34 (dd, 1H, J = 9.2, 2.8 Hz, C4-***H***), 7.09 (d, 1H, J = 9.2 Hz, C3-***H***), δ 4.01 (s, 3H, COOC***H***$_3$) ppm. ^{13}C NMR (125 MHz, $CDCl_3$) δ 169.35, 166.27, 140.09, 130.58, 126.70, 118.68, 112.18, 53.15 ppm. IR (KBr) cm^{-1}: br 3109, 1684 . HRMS *m/z* 197.0326 (M calc. 197.0324 for $C_8H_7NO_5$). Characterization data matched previously reported values.[30]

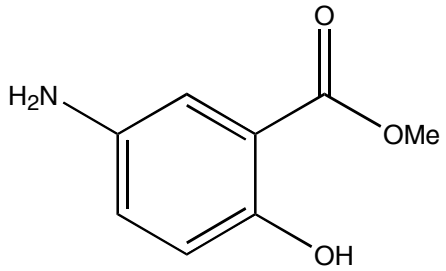

Methyl 2-Hydroxy-5-aminobenzoate **(3)**. A mixture of 3.38 g (17.2 mmol) **2** and a catalytic amount (~300 mg) of palladium on activated carbon in 180 mL of methanol was stirred at room temperature for 9 h under an atmosphere of hydrogen. The mixture was vented to ambient atmosphere and filtered to remove the catalyst. The solvent was

removed *in vacuo* to give 2.74 g (16.3 mmol) of a brown powder in 95% yield. Approximately 10 mg of **3** was recrystalized from water: m.p. 95-96 °C; ^{1}H NMR (300 MHz, CD_3OD) δ 7.22 (d, 1H, J = 2.8 Hz, C6-***H***), 6.96 (dd, 1H, J = 8.8, 2.8 Hz, C4-***H***) 6.75 (d, 1H, J = 8.8 Hz, C3-***H***), 3.89 (s, 3H, $COOCH_3$) ppm. ^{13}C NMR (125 MHz, CD_3OD) δ 170.38, 154.49, 138.81, 124.59, 117.37, 115.14, 111.91, 51.26 ppm. IR (KBr) cm^{-1}: 3412, 3323, br 3080, 1681. HRMS *m/z* 167.0580 (M, calc. 167.0582 for $C_8H_9NO_3$). Melting point matches previously reported values.[31]

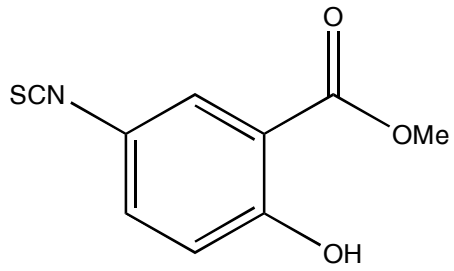

Methyl 2-Hydroxy-5-isothiocyanatobenzoate **(4)**. A solution of 4.47 g (26.8 mmol, 1 equiv.) **2** in 200 mL chloroform was added via addition funnel over 1h to a stirring mixture of 3.78 g (32.9 mmol, 1.23 equiv.) thiophosgene and 200 mL deionized water. The mixture was stirred for 6 h at room temperature. The aqueous layer was washed with 50 mL of choloform and the organic layer was washed with 2x 50 mL of deionized water. The solvent was removed *in vacuo*, affording a purple powder. The product was purified by filtration over silica gel (chloroform) to give 4.87 g (23.3 mmol) of an off white powder in 87% yield. Approximately 10 mg of **4** was recrystalized from methanol: m.p. 79-80 °C; ^{1}H NMR (300 MHz, $CDCl_3$) δ 10.8 (s, 1H, O***H***), 7.70 (d, 1H, J = 2.5 Hz, C6-***H***), 7.32 (dd, 1H, J = 8.9, 2.5 Hz, C4-***H***), 6.96 (d, 1H, J = 8.9 Hz, C3-***H***), 3.95 (s, 3H, $COOCH_3$) ppm. ^{13}C NMR (125 MHz, CDCl3) δ 169.38, 160.41, 135.40,

132.78, 126.88, 122.65, 119.09, 112.85, 52.74 ppm. IR (KBr) cm^{-1}: br 3099, 2110, 1673. HRMS *m/z* 209.0139 (M, calc. 209.0147 for $C_9H_7NO_3S$).

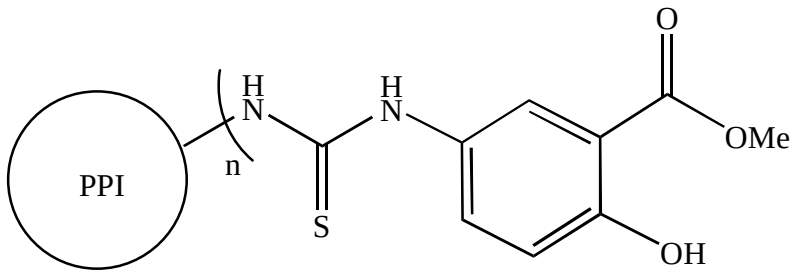

General procedure for the synthesis of functionalized PPI-based thiourea-linked Methyl 2-Hydroxy-5-thioureabenzoate dendrimers **(5a-e).** (see Table 2.2 for quantities of each component used in the series). A solution of PEI dendrimer and **4** in DMSO was stirred at room tempature for 1 h. The product was dialyzed against 9:1 DMSO-H_2O (MW cutoff 1 kDa). The solution was lyophilized to give an off white solid.

Table 2.2 Experimental Quantities for Synthesis of **5a-5e**.

Compound	Quantity of PEI mg (mmol)	Quantity of DMSO mL	Quantity of **4** mg (mmol)	% yield
5a(G1): n=4	133 (0.421)	4	520 (2.49)	20
5b(G2): n=8	167 (0.215)	4	436 (2.09)	52
5c(G3): n=16	110 (0.066)	3.5	291 (1.39)	91
5d(G4): n=32	79 (0.022)	3.5	275 (1.32)	64
5e(G5): n=64	50 (0.007)	3	118 (0.564)	85

5a: ^{1}H NMR (500 MHz, CD_3SOCD_3) δ 10.33 (bs, 1H, O***H***), 9.34 (bs, ArN***H***CSNH), 7.68 (bd, 2H, J = 2.1 Hz, ArNHCSN***H***, C6-***H***), 7.43 (app d, 1H, J = 7.6 Hz, C4-***H***), 6.91 (d, 1H, J=8.8 Hz C3-***H***), 3.84 (s, 3H, COOC***H***$_3$), 3.45 (bs, 2.5H), 2.39 (bs,), 1.62 (bs, 2.3H), 1.27 (bs, 1H,) ppm. ^{13}C NMR (125 MHz, CD_3SOCD_3) δ 181.39, 169.28, 157.68, 133.11,

131.24, 126.17, 117.94, 113.06, 53.67, 52.98, 51.46, 43.18, 26.07, 24.35 ppm. MALDI-TOF MS (pos): M_w 1156 g/mol (equivalent to 4 of **4**).

5b: ^{1}H NMR (500 MHz, CD_3SOCD_3) δ 10.33 (bs, 1H, O***H***), 9.30 (bs, ArN***H***CSNH), 7.55-7.67 (m, 1.6 H, ArNHCSN***H***, C6-***H***), 7.43 (app d, 1H, J = 7.6 Hz, C4-***H***), 6.90 (d, 1H, J = 8.5 Hz, C3-***H***), 3.83 (s, 3H, COOC***H₃***), 3.40 (bs, 1.9H), 2.39 (bs, 4.2 H), 1.25-1.58 (m, 3.5H) ppm. ^{13}C NMR (125 MHz, CD_3SOCD_3) δ 181.39, 169.34, 157.67, 133.02, 131.38, 125.95, 117.86, 112.91, 52.97, 51.78, 51.45, 43.17, 26.19 ppm. MALDI-TOF MS (pos): M_w 2451 g/mol (equivalent to 8 of **4**).

5c: ^{1}H NMR (500 MHz, CD_3SOCD_3) δ 10.33 (bs, 1H, O***H***), 9.28 (bs, ArN***H***CSNH), 7.54-7.67 (m, 2H, ArNHCSN***H***, C6-***H***), 7.42 (bs, 1H, C4-***H***), 6.91 (d, 1H, J = 8.2 Hz, C3-***H***), 3.81 (s, 3H, COOC***H₃***), 3.40 (bs, 2.0H), 2.36 (bs, 5.0H), 1.25-1.57 (m, 4H) ppm. ^{13}C NMR (125 MHz, CD_3SOCD_3) δ 181.42, 169.36, 157.66, 132.98, 131.46, 125.96, 117.75, 112.06, 52.93, 51.71, 51.46, 42.99, 26.19, 23.28* ppm. MALDI-TOF MS (pos): M_w 4200 g/mol (equivalent to 12 of **4**). *Small broad peak.

5d: ^{1}H NMR (500 MHz, CD_3SOCD_3) δ 10.34 (bs, 1H, O***H***), 9.34 (bs, ArN***H***CSNH), 7.52-7.66 (m, 2H, ArNHCSN***H***, C6-***H***), 7.42 (bs, 1H, C4-***H***), 6.85 (bs, 1H, C3-***H***), 3.80 (s, 3H, COOC***H₃***), 3.40 (bs, 3.3H), 2.33 (bs,5.4H), 1.23-1.57 (m, 24.7H) ppm. ^{13}C NMR (125 MHz, CD_3SOCD_3) δ 181.42, 169.35, 157.69, 132.99, 131.45, 125.92, 117.78, 112.85, 52.93, 51.53, 43.09, 26.23, 20.42* ppm. MALDI-TOF MS (pos): M_w 9200 g/mol (equivalent to 27 of **4**). *Small broad peak.

5e: ^{1}H NMR (500 MHz, CD_3SOCD_3) δ 10.34 (bs, 1H, O***H***), 9.29 (bs, ArN***H***CSNH), 7.65 (bs, 2H, ArNHCSN***H***, C6-***H***), 7.40 (bs, 1H, C4-***H***), 6.83 (bs, 1H, C3-***H***), 3.78 (s, 3H,

COOC***H***$_3$), 3.39 (bs, 2.5H), 2.30 (bs, 4.67H), 1.20-1.56 (m, 3.9H) ppm. ^{13}C NMR (125 MHz, CD_3SOCD_3) δ 181.38, 169.40, 157.68, 132.98, 131.37, 126.17, 117.75, 112.65, 52.90, 51.81, 51.44, 42.96, 26.16 ppm. MALDI-TOF MS (pos): M_w 16628 g/mol (equivalent to 45 of **4**).

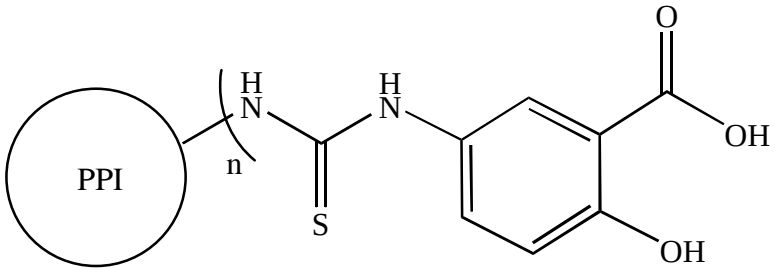

General Procedure for saponification to form functionalized PPI-based thiourea-linked 2-Hydroxy-5-thioureabenzoic acid dendrimers **(6a-e).** (see Table 2.3 for quantities of each component used in the series). A solution of LiOH in deuterium oxide (pH ~12) was added dropwise to a solution of **5** in DMSO. The solution was gently shaken and set in an oven at 55°C for 6 hours. The solution was then treated with HCl in deterium oxide (pH 0.4) to obtain ~pH 8 and then treated with HCl in deterium oxide (pH 1.4) to obtain ~pH 7.6. The mixture was lyophillized to a brown oil, reconstituted in a minimal amount of DMSO, and used without further purification. No percent yield was determined because the solvent was not totally removed from the product. Concentrations of the DMSO solution were determined using an adaptation of the no-d NMR experiment reported by Hoye and coworkers.[33,34]

Table 2.3 Experimental Quantities for Synthesis of **6a-6e**.

Compound	Quantity of **5a-e** mg (mmol)	Quantity of DMSO mL	Quantity of LiOH (pH 12) mL
6a(G1): n=4	39 (0.034)	1.3	0.4
6b(G2): n=8	124 (0.051)	4	1.3
6c(G3): n=16	150 (0.030)	4.8	1.7
6d(G4): n=32	117 (0.012)	3.7	1.2
6e(G5): n=64	85 (0.004)	2.7	0.9

6a: ^{1}H NMR (500 MHz, D_2O/CD_3SOCD_3 (1:3)) δ 7.46 (s, 1H, C6-***H***), 7.07 (bs, 1H, C4-***H***), 6.68 (d, 1H, J=7.4 Hz C3-***H***), 3.41 (bs, 1.8H), 2.97 (m, 3.8H), 1.81 (bs, 3.0H), 1.36 (bs, 0.5H) ppm. ^{13}C NMR (125 MHz, CD_3SOCD_3) δ 182.15, 172.58, 159.25, 129.86, 129.69, 127.01, 119.44, 115.84 , 67.63*, 67.47*, 50.77, 41.76, 24.21, 21.04, 20.15* ppm. Micro-TOF MS: M_W 1087 g/mol (equivalent to 4 of **4**).*Impurity peak.

6b: ^{1}H NMR (500 MHz, D_2O/CD_3SOCD_3 (1:3)) δ 7.33 (s, 1H, C6-***H***), 6.73 (bs, 1H, C4-***H***), 6.34 (s, 1H, J = 8.5 Hz, C3-***H***), 3.31 (bs, 2.1H), 2.24 (bs, 4.56 H), 1.23-1.47 (m, 3.8H) ppm. ^{13}C NMR* (125 MHz, CD_3SOCD_3) δ 182.05, 172.32, 159.52, 129.68, 126.86, 119.64, 115.71, 67.68*, 52.65*, 50.74, 24.60, 20.31 ppm. Micro-TOF MS: M_W 2312 g/mol (equivalent to 8 of **4**). *Impurity peak.

6c: ^{1}H NMR (500 MHz, D_2O/CD_3SOCD_3 (1:3)) δ 7.34 (s, 1H, C6-***H***), 6.73 (bs, 1H, C4-***H***), 6.33 (s, 1H, C3-***H***, 3.31 (bs, 1.8H), 2.20 (bs, 4.72H), 1.21-1.62 (m, 3.8H) ppm. ^{13}C NMR (125 MHz, CD_3SOCD_3) δ 182.10, 173.53, 157.34, 129.85, 129.65, 126.97, 119.42, 115.88, 112.06, 67.64*, 50.50, 23.86, 20.25 ppm. Micro-TOF MS: M_W 4795 g/mol (equivalent to 16 of **4**).*Impurity peak.

6d: ^{1}H NMR (500 MHz, D_2O/CD_3SOCD_3 (1:3)) δ 7.35 (s, 1H, C6-***H***), 6.98 (bs, 1H, C4-***H***), 6.75 (s, 1H, C3-***H***), 3.32 (bs, 1.7H), 2.23 (bs,4.7H), 1.23-1.63 (m, 3.9H) ppm. ^{13}C NMR (125 MHz, CD_3SOCD_3) δ 182.12, 172.60, 159.47, 129.84, 129.58, 127.08, 119.62, 115.87, 50.84, 41.94, 24.57, 21.21 ppm. MALDI-TOF MS (neg): M_w 9350 g/mol (equivalent to 30 of **4**).

6e: ^{1}H NMR (500 MHz, D_2O/CD_3SOCD_3 (1:3)) δ 7.65 (bs, 1H, C6-***H***), 6.54 (bs, 1H, C4-***H***), 6.41 (bs, 1H, C3-***H***), 3.33 (bs, 1.3H), 2.24 (bs, 3.9H), 1.10-1.61 (m, 3.4H) ppm. ^{13}C NMR (125 MHz, CD_3SOCD_3) δ 182.08, 172.56, 159.35, 129.71, 126.99, 119.41, 115.92, 67.66*, 50.64, 23.79, 20.30 ppm. MALDI-TOF MS (neg): M_w 15548 g/mol (equivalent to 43 of **4**). *Impurity peak.

CHAPTER THREE

PROTEIN CLEAVAGE STUDIES

Background and Rational

Dendrimers have become a popular framework on which to tether catalytic units in order to improve separation of catalyst from product. Dendrimers often have a negative impact on the catalytic activity of the monomer unit once it is bound to the dendritic framework. Frechet recently published a review of positive dendritic effects on catalytic systems.[24] The goal of this study is to synthesize generations 1-5 PPI salicyclic functionalized dendrimers and measure their activity as catalysts in the cleavage of IgG peptide backbone. If the salicylic acid endgroups display cooperativity this will be another examplein a limited number of catalytic systems enhanced by dendrimer scaffolding.

Suh and coworkers effected cleavage of IgG peptide backbone employing a PPI linear polymer functionalized with three salicylic acid residues.[25] The rate of degradation of the protein was monitored by quantification after sodium dodecyl sulfate-polyacrylamide gel electrophoresis (SDS-PAGE) analysis. The density of the electrophoretic bands was quantified by software purchased from the Jandel Corporation. Dendrimers **6a-6e** were used to promote the cleavage of IgG and were monitored in a fashion analogous to Suh's using Quantity One software from Bio-Rad.[25]

Protein Cleavage Reaction and Analysis Methods

Suh found that the most active pH range for the polymer catalyst was pH 5-7.[25] Dendrimers **6a-6e** are insoluble in aqueous solutions unless the pH is above 10.5. Since the active catalytic pH range is not contained in the soluble pH range of **6a-6e**, these compounds were used as heterogeneous catalysts. **6a-6e** were lyophilized to a gel in 5 mL flasks. IgG was dissolved in a HEPES/D_2O buffer solution at pH 7.6. D_2O was employed instead of Millipore water to ensure minimal Fe^{+3} contamination. The concentration of IgG was determined by UV absorption (ε = 1.4 ml/(mg*cm^{-1})). IgG solution and flasks containing lyophilized **6a-6e** were heated to 45 °C in an oil bath. Elevated temperatures are necessary to promote cleavage in a timely manner. During the synthesis of **6a-6e**, it was discovered that magnetic stir bars are considerable source of Fe^{+3}, hence they could not be used in the presence of **6a-6e**. A carousel was engineered to stir 4 flasks simultaneously in an oil bath and to minimize localized high activity of **6a-6e** in the buffer solution. An aliquot was taken immediately upon addition of IgG solution to dendrimer. Subsequent aliquots were taken over a 24 hr period. Aliquots were placed in a refrigerator at 4 °C to arrest cleavage. After all aliquots were collected and chilled in the refrigerator, the samples were warmed, treated with SDS sample buffer, and then vortexed. The SDS buffer recipe is included in the experimental section of this chapter. The samples were heated to 95 °C for 5 min, vortexed and centrifuged for 15 s. The samples were loaded onto Bio-Rad 10% Tris HCl precast polyacrylamide electrophoresis gels. Gels were soaked in 10% methanol and 7% acetic acid for 1 h to set the protein bands, followed by soaking in Sypro Ruby for 8 h to stain the bands, and soaked in 10%

methanol and 7% acetic acid for 36 h to destain the bands. Resulting electrophoretic bands were quantified using Quantity One software and a Molecular Imager FX scanner, both from Bio-Rad. A more detailed explanation of the Quantity One analysis is included in the experimental section of this chapter.

Errors in Quantitative SDS-PAGE Analysis

Certain errors are unavoidable when analysis by SDS-PAGE is employed in a study and the errors can have a cumulative effect. The chronologically first source of error is measuring the 20 μL aliquots from the original reaction mixture with Hamilton syringes. One or two μL difference could easily have a pronounced effect on the density of the corresponding electrophoretic band. The second obvious source of error is the physical loading of aliquots into the gel wells. The same Ranin Pipeteman was used for all the gels. The volume was always set at 10 μL and the air purge was not used. However, inconsistent delivery is not completely avoidable. Inconsistent cross-linking of the polyacrylamide of the gels is a potential cause of band broadening and overlap. Overlap of bands could also have been induced by a small leak in the SDS-PAGE running cell. Bands at the edge of the gel were on occasion obviously imperfect and not reliable for accurate data. In some cases, contaminant smearing into the bands occurred perhaps due to the handling of the gels during staining and destaining. Indeterminant errors present themselves in the form of electrophoretic bands that are grossely removed from the trend in a given gel. All unreliable bands were identified and were not used in quantitative analysis. Aliquots taken at times later than 12 hours were sometimes more

concentrated than expected. This was attributed to solvent evaporation through comprimised septa. The most prominent source of error was handling induced smearing and late time point increase in concentration.

Qualitative Analysis of Protein Cleavage Studies

Visual inspection of the SDS-PAGE gels, using the Molecular Imager FX from Bio-Rad, revealed an evident decrease in the volume of the bands of the reaction of IgG with **6e**. Tables of volume counts for the individual electrophoretic bands are necessary to find trends in the reactions of IgG with **6a-6d** and unbound salicylic acid as volume changes in the gel bands are less obvious. The volume of the bands is equal to the pixel count inside a boundary multiplied by the area of the boundary. The volumes of the various bands at different time periods will be referred to as U1-15. The units of time are hours. Each gel (except the gels for **6d**) was loaded with 4 standard dilutions of IgG with no dendrimer (S1, S2, S3, and S4) for quantification if found applicable. The concentration of a stock IgG solution (S1) was determined by UV spectroscopy. S2, S3, and S4 are the result of a 1:1 serial dilution of S1. IgG has a pair of heavy chains and a pair of light chains. Theoretically, the heavy chain could be cleaved into pieces roughly equivalent to the light chain. In this study only degradation of the heavy chain is discussed. Figures 3.1-3.3 show the gels of trials 1-3, respectively, of the reaction of **6e** and IgG. Trial 1 and 2 (Fig. 3.1 and Fig 3.2 respectively) have significant smearing and overlap of the bands making quantification more complicated. The bands are different shapes hence the area and pixel count of the bands must be determined. Trial 2 has

severe smearing and was not quantitatively evaluated. The steps taken to quantify the gels are explained in the Quantitative Analysis section of Chapter 3. An obvious decrease in the volume of the bands was seen as time increases. This means that the concentration of the heavy chain of IgG is decreasing over time because it is being cleaved by **6e**. Henceforth the concentration of the heavy chain of IgG will be referred to as the concentration of IgG. Bands U8 and U9 of Fig. 3.2 were disregarded due to contaminant smearing. Trial 3 (Fig 3.3) shows a steady decrease in the concentration of IgG with uniform and well behaved electropheritic bands. Bands U11 and U15 were disregarded due to edge effects. The uniform bands allow quantification with simply the volume measurement. The rate constants for reactions shown in Fig. 3.1 and Fig. 3.3 are in the Quantitative Analysis section of Chapter 3.

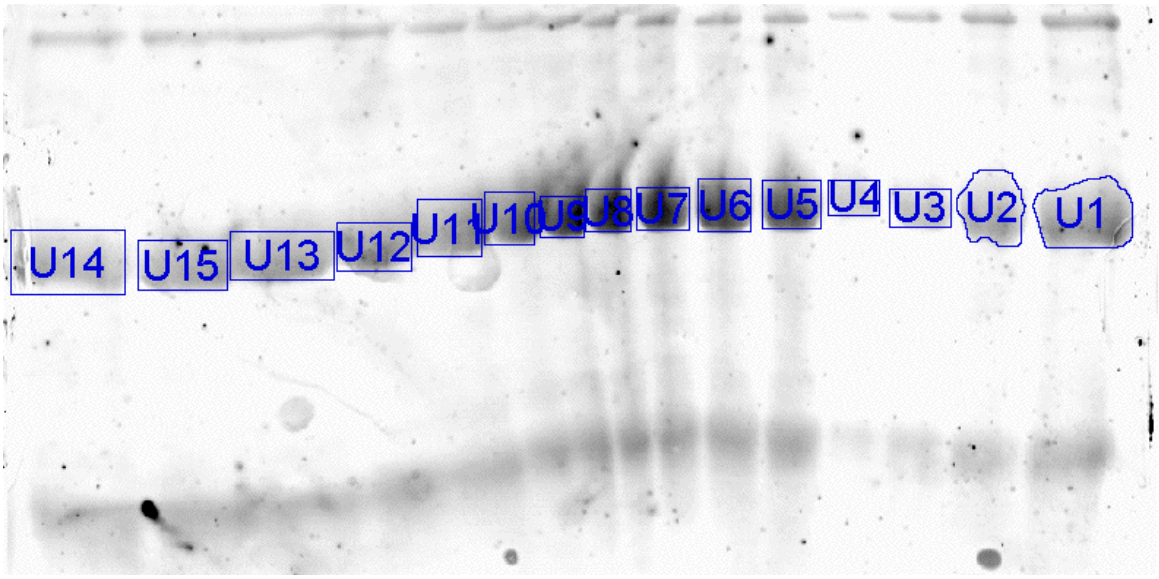

Figure 3.1 Trial 1 electrophoretic gel of IgG with **6e.**

Table 3.1 Quantitation of Figure 3.1 using Quantity One software.

Name	Volume CNT*mm2	Density CNT/mm2	Area mm2	CNT	Time h
U1	56686.43591	149017.9392	0.616765822	91909.17181	S1
U2	27307.51285	105231.2414	0.509411478	53606.00225	S2
U3	14028.57146	90506.89379	0.393700435	35632.60343	S3
U4	9262.310966	77899.99187	0.344818829	26861.38397	S4
U5	44954.98469	245253.5478	0.428135537	105001.7594	0.00
U6	48532.92506	262481.9629	0.430000045	112867.2558	1.00
U7	45189.47471	307411.3285	0.38340583	117863.2956	2.00
U8	40820.20426	333498.3312	0.34985715	116676.7758	3.00
U9	39787.57415	344481.0896	0.339852945	117072.9127	4.00
U10	40179.43419	239163.2489	0.409878073	98027.77167	5.00
U11	39661.24414	165807.8422	0.489080821	81093.43568	6.50
U12	40235.3242	171945.794	0.483735515	83176.28729	7.50
U13	45392.22473	140229.2717	0.568946454	79782.94691	8.50
U14	41940.76437	87668.80356	0.691664731	60637.41942	21.00
U15	40154.95419	139426.8952	0.536656371	74824.33153	9.50

Figure 3.2 Trial 2 electrophoretic gel of IgG with **6e** and quantification**.**

Table 3.2 Quantitation of Figure 3.2 using Quantity One software.

Name	Volume CNT*mm2	Density CNT/mm2	Area mm2	CNT	Time h
U1	86221.52615	279940.045	0.554977452	155360.4129	S1
U2	46796.86791	163854.5942	0.534415545	87566.4422	S2
U3	18217.61919	95180.882	0.437492838	41640.95414	S3
U4	16027.73928	80500.95789	0.44620621	35920.02735	S4
U5	50543.65774	203969.5814	0.497795116	101535.0615	0
U6	40695.87818	153801.5186	0.514392823	79114.39733	1
U7	49288.1378	202000.5828	0.493963539	99780.92283	2
U8	61948.28723	241325.6438	0.506655679	122269.0079	3
U9	70811.10683	258623.4959	0.523258995	135327.0704	4
U10	53196.10762	209433.5133	0.503984104	105551.1616	5
U11	67204.527	262928.5329	0.505568964	132928.5059	6.5
U12	63275.09717	224379.7973	0.531036698	119153.9067	7.5
U13	62506.47721	190743.0052	0.572450846	109190.9946	8.5
U14	46508.35792	140085.4279	0.576194386	80716.43713	9.5
U15	49322.2678	137311.4482	0.599332936	82295.27338	21

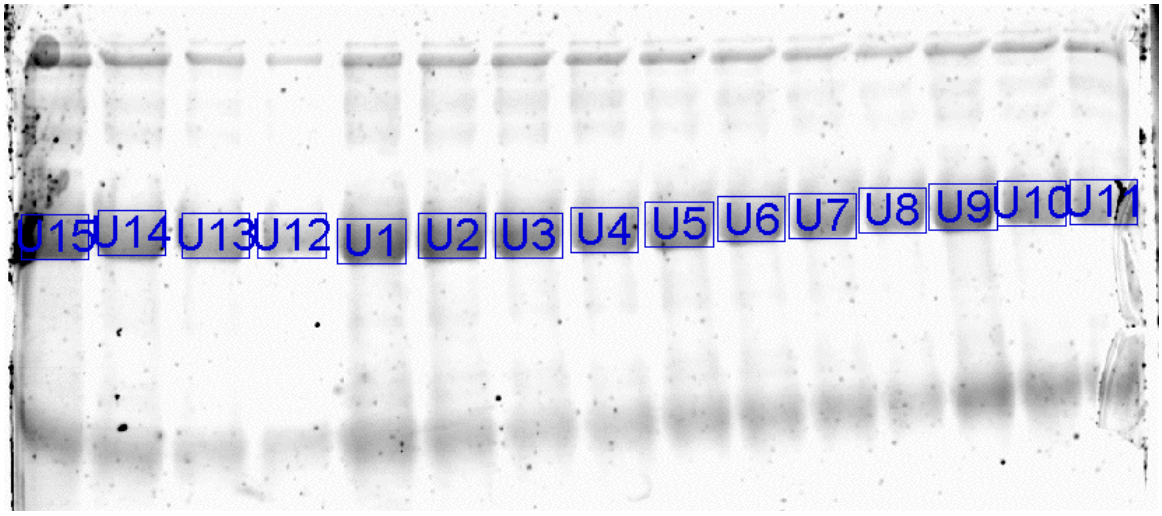

Figure 3.3 Trial 3 electrophoretic gel of IgG with **6e.**

Table 3.3 Quantitation of Figure 3.3 using Quantity One software

Name	Volume CNT*mm2	Time h
U1	82814.10247	0.00
U2	84018.6525	1.00
U3	76641.90228	2.00
U4	62648.90187	3.00
U5	65182.65194	4.00
U6	56911.4617	5.00
U7	58495.31174	6.50
U8	47152.66141	7.50
U9	73200.18218	8.50
U10	56991.9617	9.50
U11	70179.20209	21.00
U12	34734.44104	S4
U13	49474.16147	S3
U14	68907.03205	S2
U15	126501.5438	S1

The gels for the 3 trials of the reaction of **6d** and IgG are shown in Figures 3.4-3.6. Trial 1 (Fig 3.4) has no standards. S1 was the only standard loaded and it was disregarded due to edge effects. Visual analysis of the volumes of the bands does not reveal a trend as clearly as in the reactions with **6e**. The volume measurements afforded by Quantity One can be used as a rough guide to the catalytic activity of the dendrimer since the bands are not overlapping. U4 and U5 should be expelled because both are clearly erroneous in comparison to neighbors. The trend in Table 3.4 reveals a slight decrease in the concentration of IgG.

Trial 2 (Fig 3.5) offers no evident trend from visual inspection. Table 3.5 shows no obvious decrease in IgG concentration over time. Instead, a slight increase in IgG concentration is seen. Due to unknown experimental error, U3 does not follow the trend and should be discarded. This increase in concentration is resultant of either evaporation of buffer through compromised septa or unavoidable errors inherent in this methodology.

Trial 3 (Fig. 3.6) has a large smear on U1, U2, U12 and U13. Visual analysis of U3-U11 shows an obvious decrease in the concentration of IgG. **6d** was not analyzed for rate data. Trial 3 being the most promising showed a decrease in concentration of IgG late in the assay. More data points later in the time line would be necessary to accurately display the concentration decrease. This was not possible given the frequency of solvent evaporation and increasing concentrations of IgG.

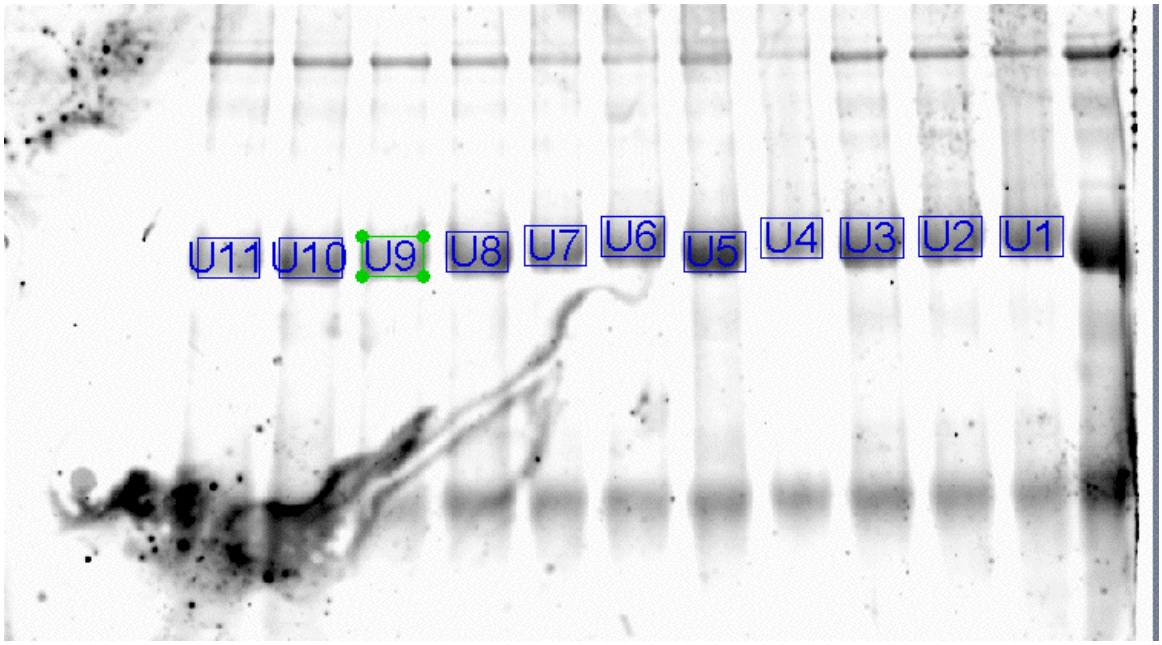

Figure 3.4 Trial 1 electrophoretic gel of IgG with **6d.**

Table 3.4 Quantitation of Figure 3.4 using Quantity One software

Name	Volume CNT*mm2	Time h
U1	71162.89742	0.00
U2	70374.21734	0.50
U3	74583.26778	1.00
U4	48133.38502	1.50
U5	95240.00993	2.00
U6	55850.44583	3.00
U7	55574.4358	4.75
U8	70854.86739	7.50
U9	53258.83556	8.50
U10	64147.82669	10.50
U11	43217.31451	22.50

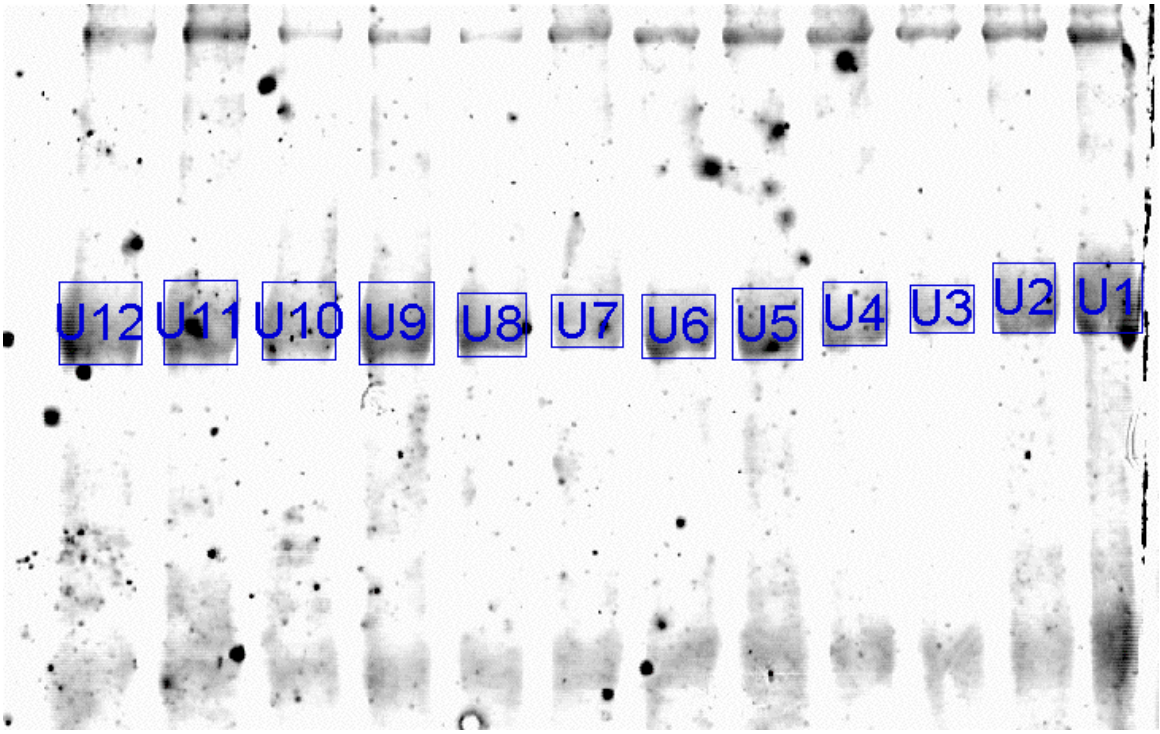

Figure 3.5 Trial 2 electrophoretic gel of IgG with **6d.**

Table 3.5 Quantitation of Figure 3.5 using Quantity One software.

Name	Volume CNT*mm2	Density CNT/mm2	Area mm2	CNT	Time h
U1	69491.08725	301741.523	0.479895872	144804.5113	S1
U2	41212.5543	195598.2235	0.459020745	89783.64221	0
U3	16580.29173	114189.3132	0.381051217	43511.97679	0.5
U4	32477.94339	160384.8722	0.450000047	72173.2	1
U5	50970.43532	212376.7695	0.489898	104042.9546	1.5
U6	44312.12462	201418.7063	0.469041625	94473.75727	2
U7	27140.45283	149699.1019	0.425793422	63740.89279	3
U8	42482.63443	205428.5569	0.454752727	93419.19655	4.75
U9	65211.9068	220013.1349	0.54442636	119780.9503	7.5
U10	46897.51489	167192.5316	0.529622562	88548.93698	8.5
U11	68746.16717	233037.8062	0.543139081	126571.9399	10.5
U12	70344.28734	212777.5943	0.57497832	122342.5038	22.5

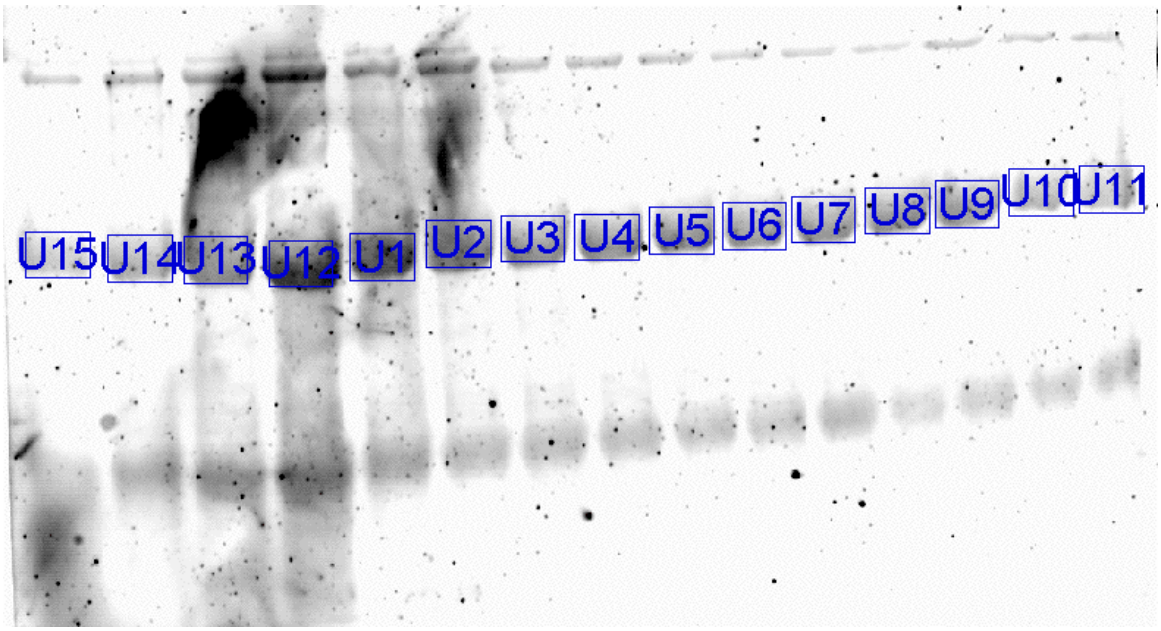

Figure 3.6 Trial 3 electrophoretic gel of IgG with **6d.**

Table 3.6 Quantitation of Figure 3.6 using Quantity One software.

Name	Volume CNT*mm2	Time h
U1	90829.49271	0.00
U2	74037.09221	1.00
U3	46197.33138	2.00
U4	45489.79136	3.00
U5	47192.62141	4.00
U6	39897.88119	5.00
U7	38814.15116	6.00
U8	44246.53132	7.00
U9	41668.68124	8.00
U10	21626.10064	10.00
U11	23543.7507	22.00
U12	95985.00286	S1
U13	65657.42196	S2
U14	36205.13108	S3
U15	21325.23064	S4

The results of the reaction of IgG and **6c** are shown in Figures 3.7-3.9 and Tables 3.7-3.9. Trial 1 (Fig. 3.7) at initial analysis shows minimal change in band intensity. Table 3.7 shows, after disregarding U7, U8, and U9 for thumb smearing, no significant decrease in IgG concentration as occurred. Trial 2 (Fig 3.8) produced similar results to Trial 1. Table 3.8 with removal of U14 for edge effects shows no decease in the concentration of IgG. Trial 3 (Fig 3.9) has no trends evident upon visual analysis. Disregarding U6, U7, U8, and U9 for smearing, Table 3.9 shows a general trend of stable volumes of the electropheretic bands. No significant decrease in the concentration of IgG is evident in any of the trials. Dendrimer **6c** displays no activity in the catalysis of the cleavage of the IgG peptide backbone under the given experimental conditions

The results of the reaction of IgG with **6b** are seen in Figures 3.10-3.12 and Table 3.10-3.12. As with Figures 3.7-3.9, no evident change in IgG concentration can be seen solely from visual inspection. Analysis of Tables 3.10-3.12 offer no decrease in the concentration of IgG The bands omitted for smearing are U12, U13, and U14 of Fig. 3.10. U7, U8, U9, and U10 bands of Fig. 3.11 were also omitted for smearing. Lastly, bands U13 and U14 of Fig. 3.12 were omitted for smearing. Dendrimer **6b** displays no activity in the catalysis of the cleavage of the IgG peptide backbone under the given experimental conditions.

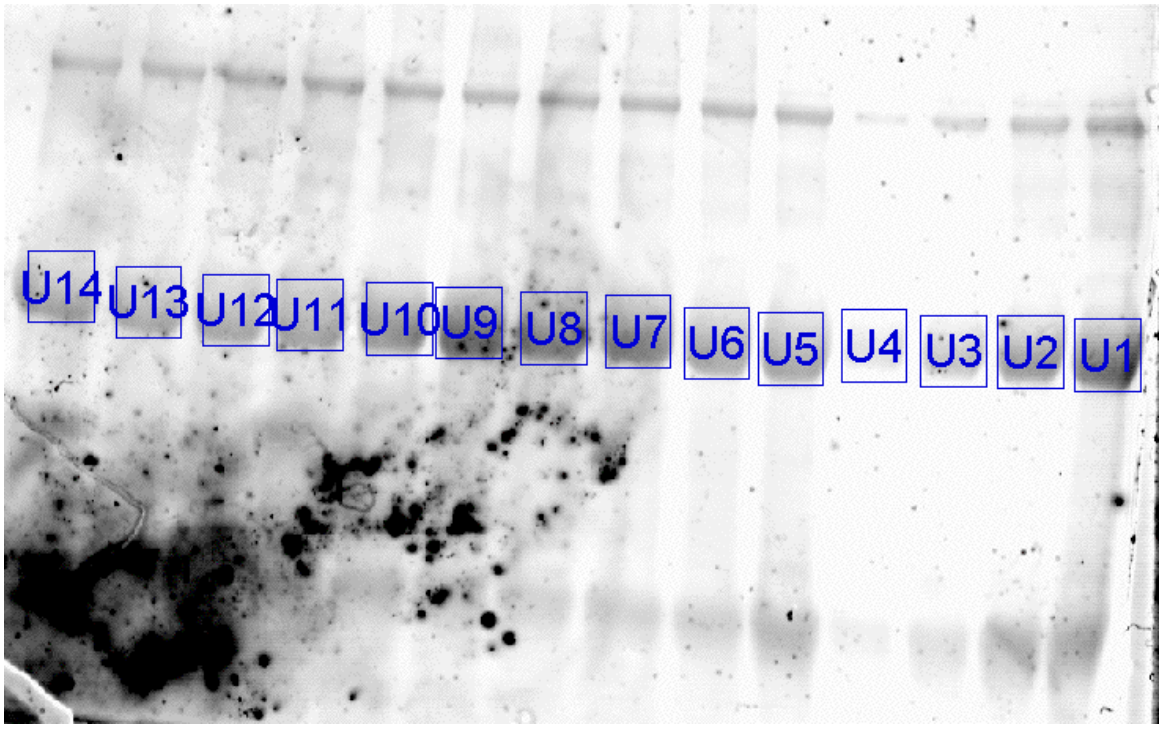

Figure 3.7 Trial 1 electrophoretic gel of IgG with **6c.**

Table 3.7 Quantitation of Figure 3.7 using Quantity One software.

Name	Volume CNT*mm2	Time h
U1	81872.06244	S1
U2	50023.76149	S2
U3	24120.30072	S3
U4	9384.17028	S4
U5	44301.75132	0.00
U6	45262.30135	1.00
U7	74586.55222	2.00
U8	86567.15258	3.00
U9	87387.8026	4.33
U10	59528.44177	5.33
U11	56619.09169	6.33
U12	45673.82136	7.33
U13	50205.9315	8.33
U14	51974.22155	20.5

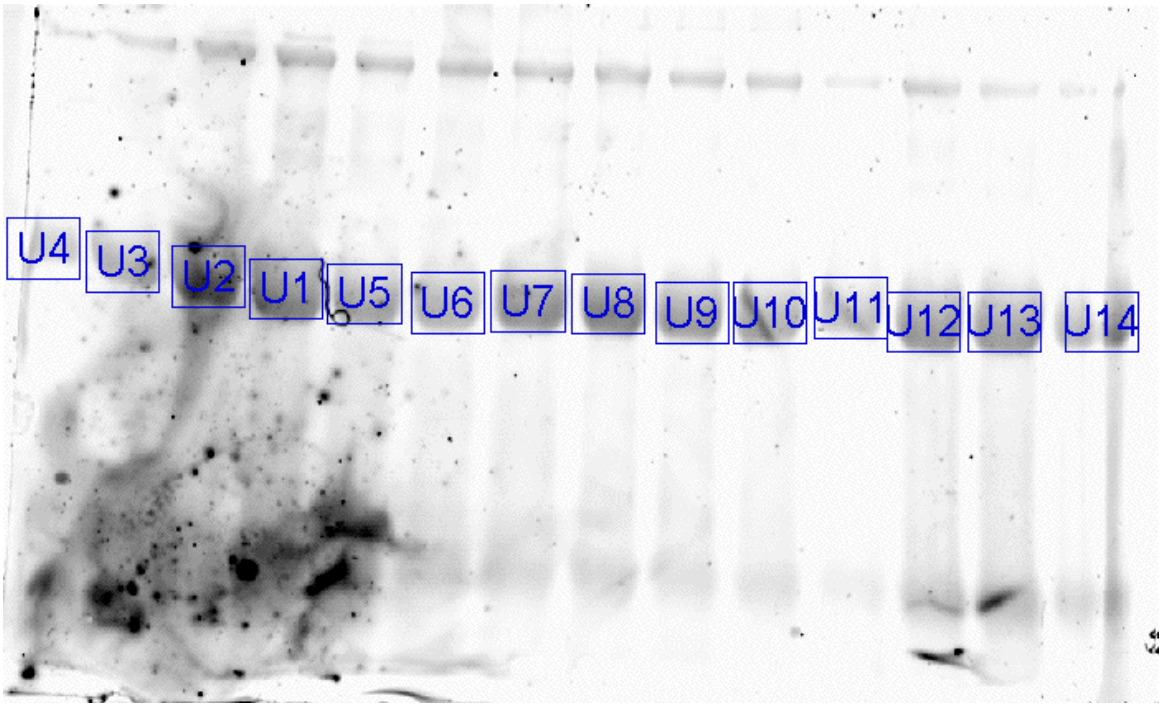

Figure 3.8 Trial 2 electrophoretic gel of IgG with **6c.**

Table 3.8 Quantitation of Figure 3.8 using Quantity One software.

Name	Volume CNT*mm2	Time h
U1	143912.035	S1
U2	193535.8602	S2
U3	72355.02755	S3
U4	28770.103	S4
U5	92252.07962	0.00
U6	72356.13755	1.00
U7	105340.951	2.00
U8	101516.1706	3.00
U9	84968.34886	4.33
U10	80796.73843	5.33
U11	49929.18521	6.33
U12	88867.82927	7.33
U13	91943.02959	8.33
U14	67310.37702	20.5

Figure 3.9 Trial 3 electrophoretic gel of IgG with **6c.**

Table 3.9 Quantitation of Figure 3.9 using Quantity One software.

Name	Volume CNT*mm2	Time h
U1	74277.53221	21.00
U2	86948.99259	9.33
U3	83939.8225	8.33
U4	105412.0131	7.33
U5	96430.50287	6.33
U6	106268.1832	5.00
U7	57472.60171	4.00
U8	84641.53252	3.00
U9	82860.64247	2.00
U10	58837.04175	1.00
U11	44011.81131	0.00
U12	45953.96137	S1
U13	23869.60071	S2
U14	14986.32045	S3
U15	8328.420248	S4

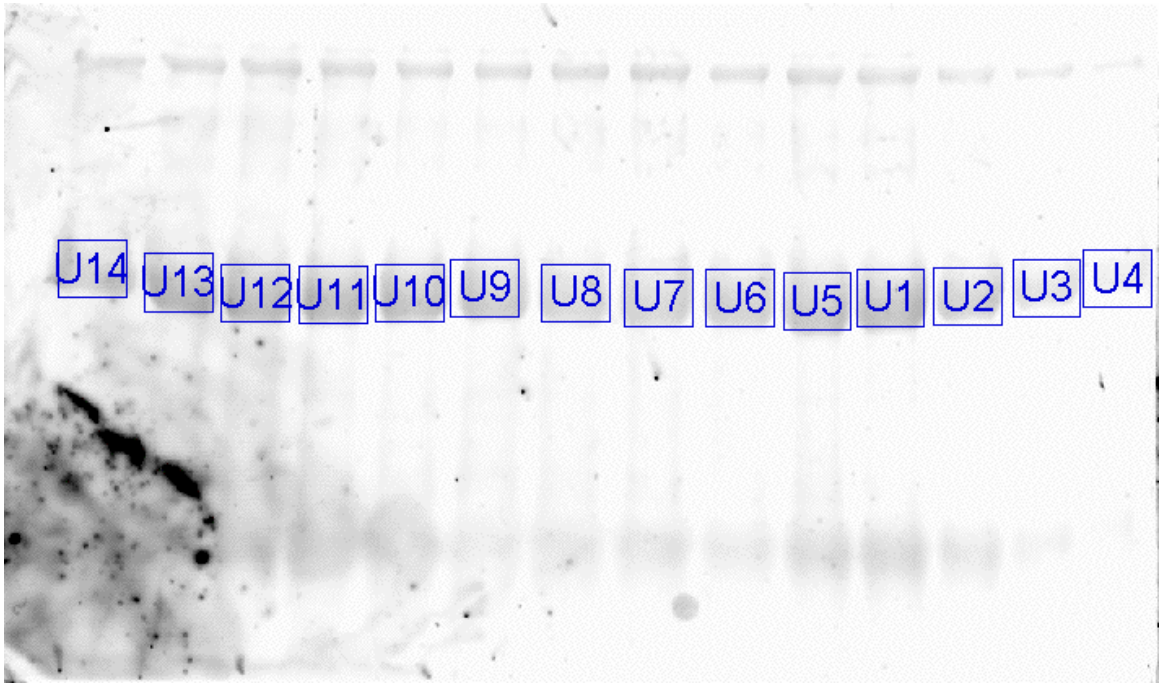

Figure 3.10 Trial 1 electrophoretic gel of IgG with **6b.**

Table 3.10 Quantitation of Figure 3.10 using Quantity One software.

Name	Volume CNT*mm2	Time h
U1	86057.67898	S1
U2	53063.59553	S2
U3	27189.79284	S3
U4	13216.68138	S4
U5	74913.00781	0
U6	63437.04662	1
U7	60129.19627	2
U8	54248.35566	3
U9	62079.00648	4.33
U10	79357.02828	5.33
U11	90985.42949	6.33
U12	100802.1205	7.33
U13	102574.3807	8.33
U14	76584.90799	20.5

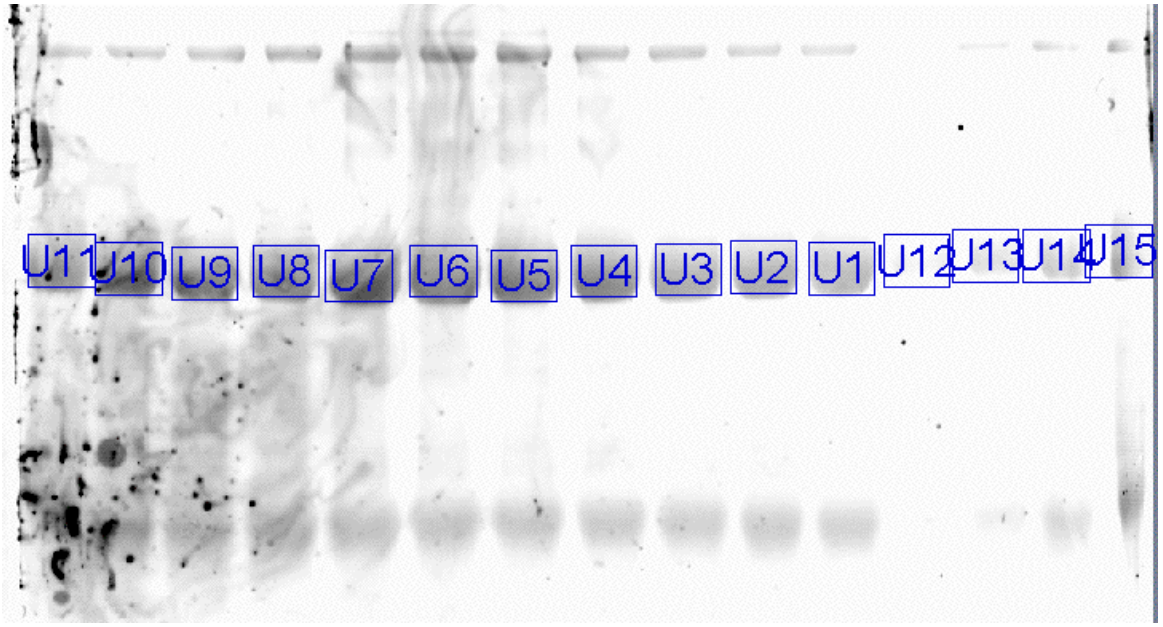

Figure 3.11 Trial 2 electrophoretic gel of IgG with **6b.**

Table 3.11 Quantitation of Figure 3.11 using Quantity One software.

Name	Volume CNT*mm2	Time h
U1	33595.2585	0.00
U2	40612.50818	1.00
U3	43066.66807	2.00
U4	61774.62724	3.00
U5	74851.86665	4.00
U6	74210.58668	5.00
U7	85151.87619	6.50
U8	67923.30696	7.50
U9	72841.59674	8.50
U10	89447.596	9.50
U11	56759.16746	21
U12	1730.159923	S4
U13	7072.269684	S3
U14	11188.4495	S2
U15	15360.32931	S1

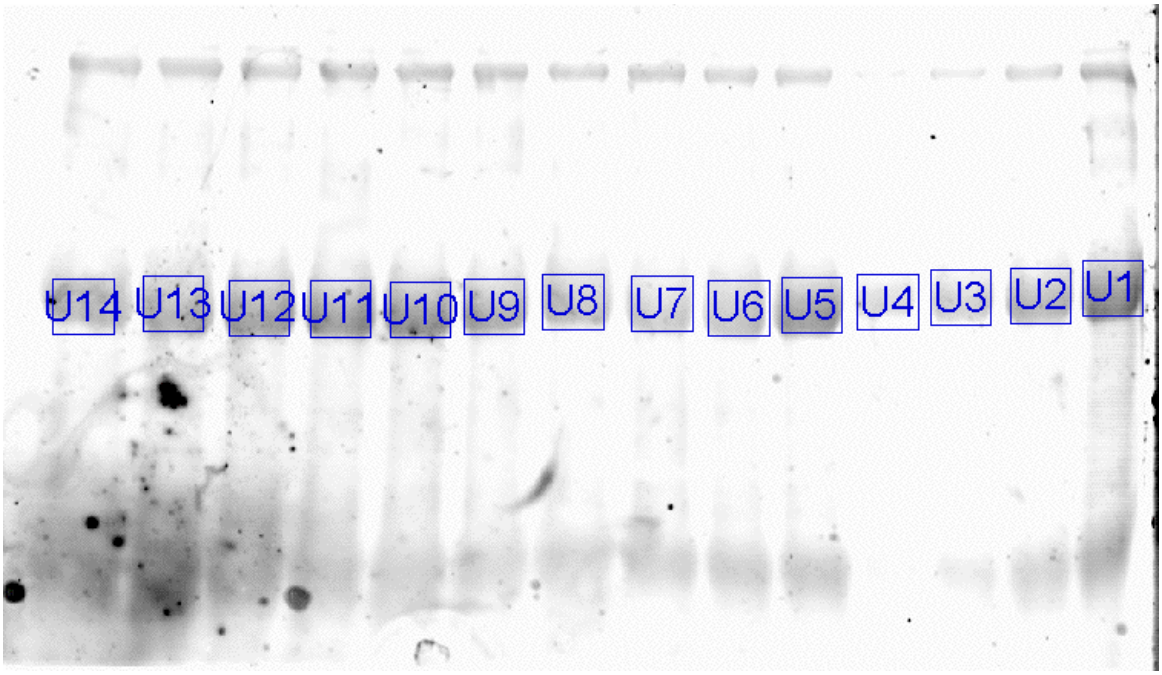

Figure 3.12 Trial 3 electrophoretic gel of IgG with **6b.**

Table 3.12 Quantitation of Figure 3.12 using Quantity One software.

Name	Volume CNT*mm2	Time h
U1	75037.19224	S1
U2	42096.87125	S2
U3	22765.21068	S3
U4	13384.8304	S4
U5	59320.41177	0.00
U6	34082.88102	1.00
U7	27604.12082	2.00
U8	39031.61116	3.00
U9	50254.0515	4.33
U10	68410.30204	5.33
U11	65340.63195	6.33
U12	62686.74187	7.33
U13	54840.81163	8.33
U14	49369.60147	20.50

Results of the reaction of IgG with **6a** are displayed in Figure 3.13 and Figure 3.14. Visual inspection of the gels reveals minimal change in the intensity of the bands and hence minimal change in the concentration of IgG. Table 3.13 and Table 3.14 show no significant change in the concentration of IgG. Band U13 in Fig. 3.13 was omitted for edge effects. Bands U9 and U10 in Fig. 3.14 were disregarded for edge effects and severe difference from the obvious trend, respectively. **6a** shows no significant catalytic activity in the cleavage of the IgG peptide backbone under the experimental conditions.

Figure 3.15 and Figure 3.16 show the results of the reaction of IgG with **1**. Trial 1 (Fig. 3.15/Table 3.15) shows no significant decrease in the concentration of IgG when excluding bands U8, U9, and U10 for smearing. Trial 2 (Fig. 3.16/Table 3.16) suffers

band overlap similar to Fig. 3.1a and Fig. 3.1b making use of the quantification in Table 3.16 less reliable. Visual inspection offers no noticeable decrease in band volume.

Figure 3.17 shows the results of the reaction of IgG and **7**. Visual inspection shows a noticeable decrease in the intensity of the bands. Table 3.17 confirms this trend. **7** appears to effectively enhance the cleavage of the IgG peptide backbone. Only one trial with **7** was completed. Further exploration would be necessary to conclusively identify the catalytic activity of **7**, but was not undertaken at this time.

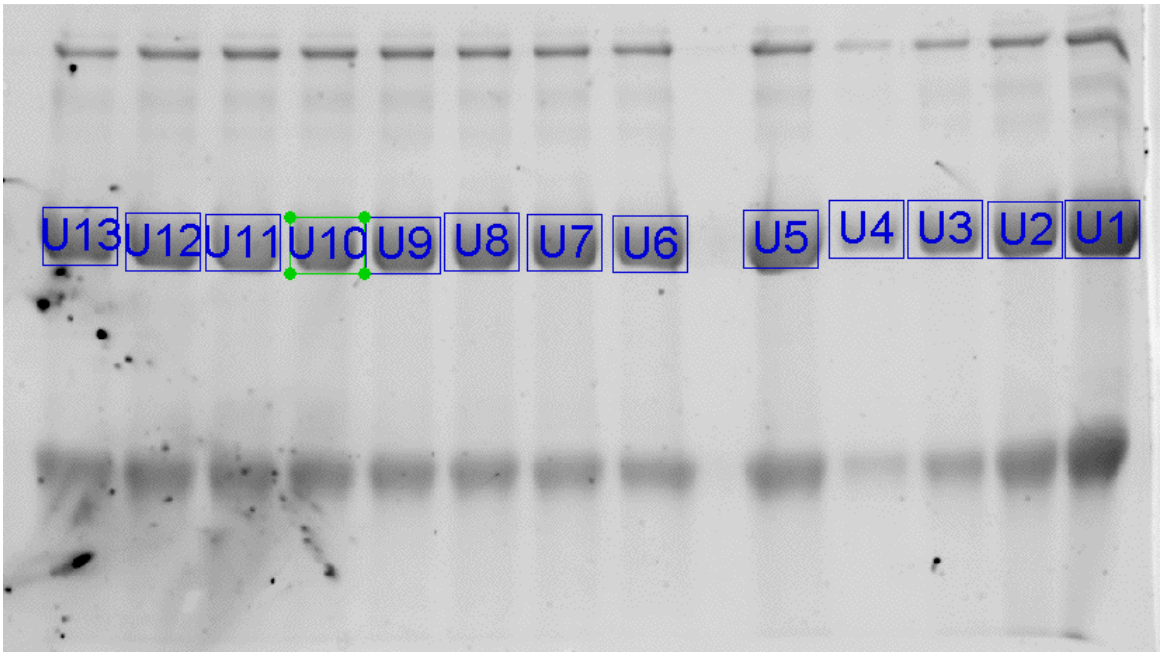

Figure 3.13 Trial 1 electrophoretic gel of IgG with **6a.**

Table 3.13 Quantitation of Figure 3.13 using Quantity One software.

Name	Volume CNT*mm2	Time h
U1	592394.7277	S1
U2	471772.0741	S2
U3	397668.2519	S3
U4	329798.1098	S4
U5	488794.7846	0.00
U6	461107.1237	2.00
U7	467537.9639	4.00
U8	459724.0237	5.00
U9	467334.3639	6.00
U10	458294.4037	7.00
U11	438157.5431	8.00
U12	479587.2543	10.00
U13	505425.7851	20.00

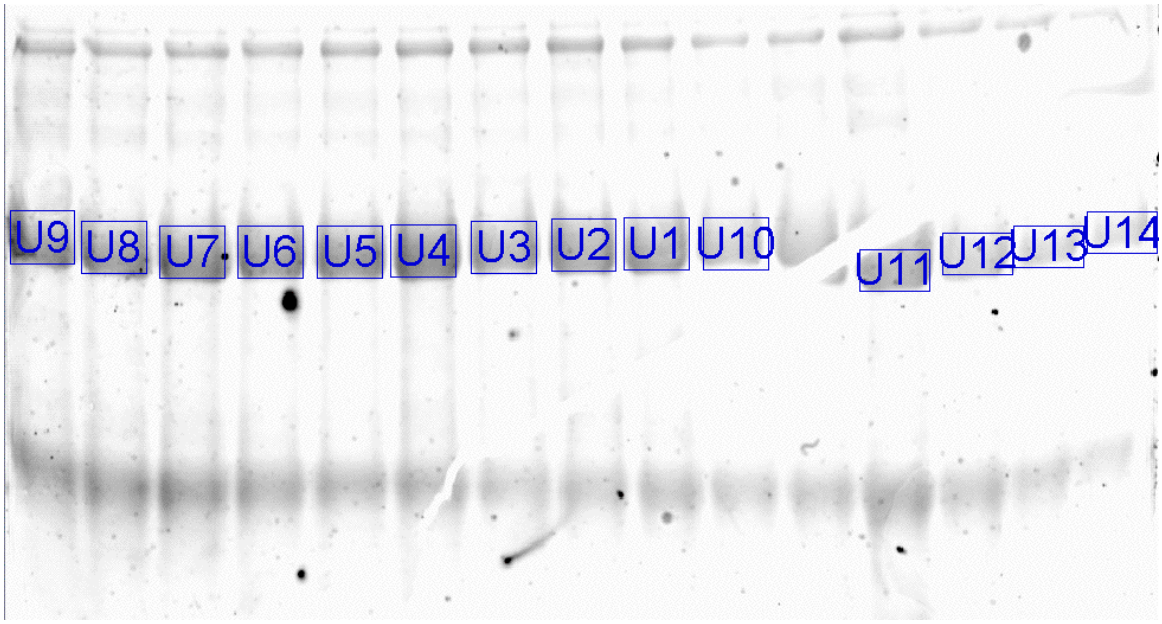

Figure 3.14 Trial 2 electrophoretic gel of IgG with **6a.**

Table 3.14 Quantitation of Figure 3.14 using Quantity One software.

Name	Volume CNT*mm2	Time h
U1	42473.38127	2
U2	49030.63146	3
U3	44543.92133	4
U4	65779.55196	5
U5	57198.8317	6
U6	55069.89164	7
U7	62790.97187	8
U8	55591.31166	16
U9	62781.11187	20
U10	24520.33073	1
U11	38380.30114	S1
U12	20394.89061	S2
U13	12119.80036	S3
U14	9442.590281	S4

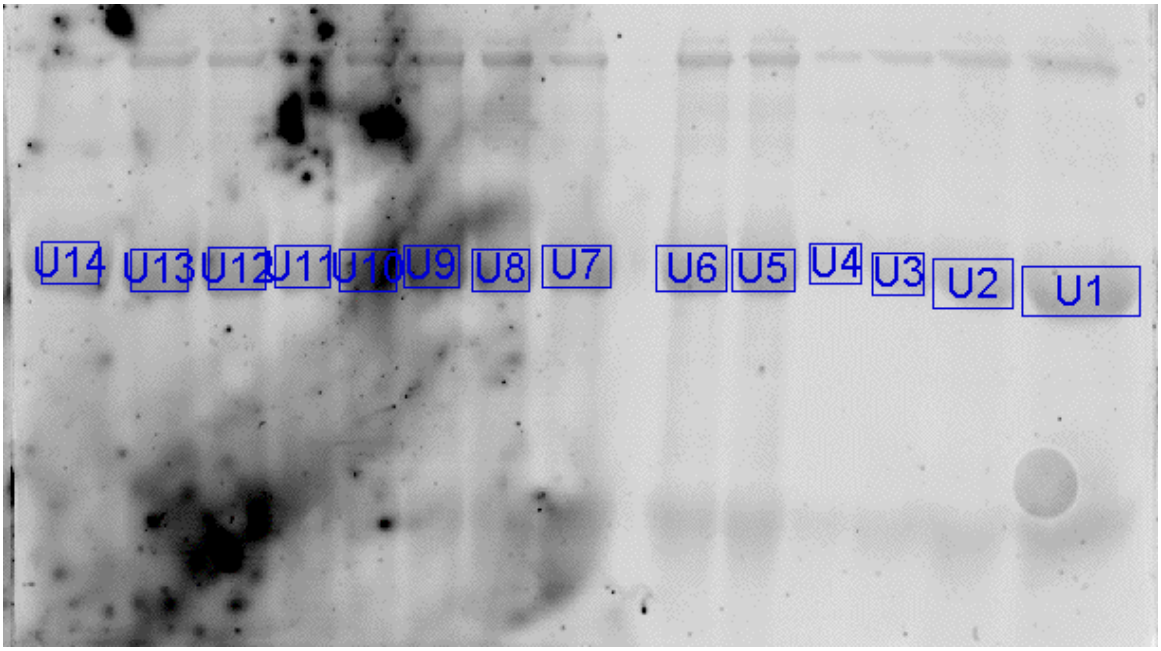

Figure 3.15 Trial 1 electrophoretic gel of IgG with **1.**

Table 3.15 Quantitation of Figure 3.15 using Quantity One software.

Name	Volume CNT*mm2	Time h
U1	492663.7747	S1
U2	322603.2296	S2
U3	160379.5248	S3
U4	144896.0343	S4
U5	246029.0073	0.00
U6	303248.169	1.00
U7	302954.009	2.00
U8	287801.4486	4.00
U9	390123.5516	5.00
U10	419249.7725	6.00
U11	241812.9172	7.00
U12	264877.5479	8.00
U13	265748.3779	16.00
U14	238752.8971	20.00

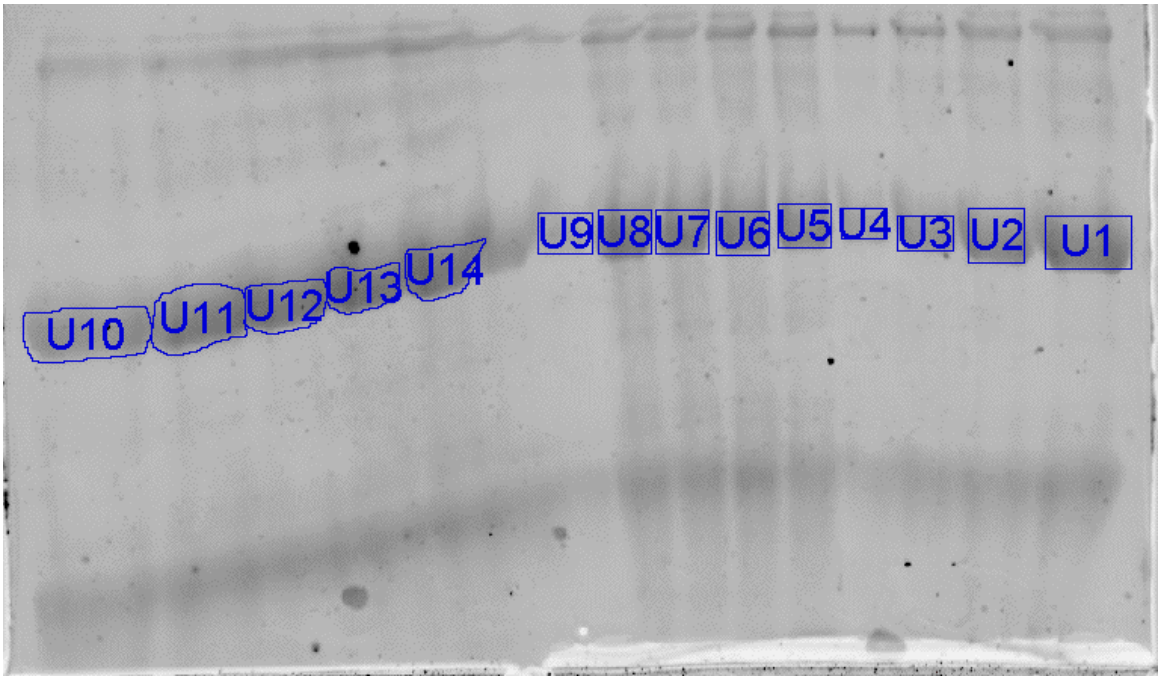

Figure 3.16 Trial 2 electrophoretic gel of IgG with **1**

Table 3.16 Quantitation of Figure 3.16 using Quantity One software.

Name	Volume CNT*mm2	Time h
U1	302176.709	S1
U2	199005.8859	S2
U3	121602.2536	S3
U4	79913.37238	S4
U5	151875.2745	0.00
U6	153631.4346	1.00
U7	155604.4046	2.00
U8	161650.7948	3.00
U9	124530.5237	4.00
U10	381605.6814	6.00
U11	357956.6907	7.00
U12	264205.5779	8.00
U13	212875.7263	16.00
U14	238861.3571	20.00

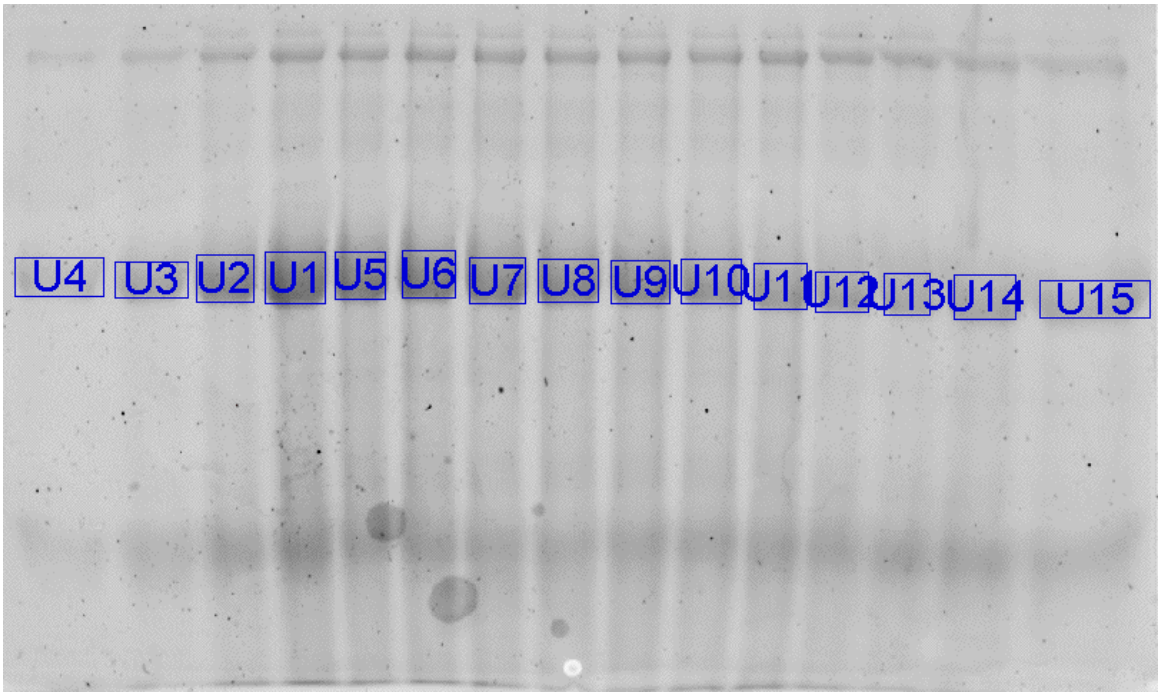

Figure 3.17 Trial 1 electrophoretic gel of IgG with **7**

Table 3.17 Quantitation of Figure 3.17 using Quantity One software.

Name	Volume CNT*mm2	Time h
U1	264083.4779	S1
U2	205710.0761	S2
U3	168323.395	S3
U4	196658.1759	S4
U5	198584.0859	0.00
U6	208351.8762	1.00
U7	203083.3161	2.00
U8	201409.476	3.00
U9	201146.366	4.00
U10	187728.7356	5.00
U11	163442.7749	6.00
U12	139500.7542	7.00
U13	123948.7837	8.00
U14	178261.2253	16.00
U15	258010.1077	20.00

Summary of Qualitative Analysis

Cleavage of the IgG peptide backbone was catalytically enhanced by **6d, 6e**, and **7**. **6a**, **6b, 6c,** and **1** displayed no noticeable catalytic activity under the experimental conditions of this study. Dendrimer **6e** will be quantitatively evaluated and a rate law will be computed. Dendrimer **6d** will not be quantitatively evaluated given the slower nature of its activity.

Quantitative Analysis.

Each gel has a set of standards of known concentration resulting from a 1:1 serial dilution of the stock solution for quantitative purposes. The theoretical concentration of

the standards are S1= 100%, S2=50%, S3=25%, and S4=12.5%. The volumes of the bands of the standards should also decrease at the same rate, but this is not the case. A correction equation was generated by plotting the experimental volume percentages of the bands versus the theoretical volume percentages of the bands. All the experimentally determined volumes of the bands were adjusted by this formula. However, if the bands of the gel are not uniform in shape and size then the volume must be converted to the pixel count. This is accomplished by finding the area of the band. The area is found by taking the square root of the quotient of the area over the density. The pixel count is then determined by multiplying the density by the area. The same procedure described above for generating an adjustment formula for the bands was also done for the pixel counts of gels with nonuniform bands. The adjusted volumes/pixel counts were converted to concentration using the ratio of the concentration of the concentrated standard used and the volume of the corresponding band after adjustment by the aforementioned formula. The concentrations were loaded with the corresponding time points into the Gesapi Biochemical Kinetic Simulator program to generate a rate law using the catalytic activator kinetic model. Figure 3.18 and 3.19 show a graph of the data and curve generated by Gepasi to fit the data for **6e** Trial 1 and Trial 3 respectively. Trial 2 was not analyzed given the severe overlap of the bands. The rate law generated for **6e** Trial 1 is: $r=3.12x10^{-2}[SaI][IgG]$. The rate law generated for **6e** Trial 3 is $r=7.04x10^{-2}[SaI][IgG]$. The average rate constant for the hydrolysis of the heavy chain of IgG by **6e** is k1=5.08e-2 ± 0.02. Given the rate laws and the qualitative data from the SDS-PAGE studies, a

generation 5 salicylic acid functionalized dendrimer effectively catalyzes the cleavage of the IgG peptide backbone.

Suh and Hah explored the pH range for the activity of their catalyst. They determined that in the active pH range the phenol of SaI is protonated and the carboxylate is deprotonated. They found a rate constant for the cleavage of the heavy chain of IgG by the active form of the catalyst. $k_1 = 0.43 \pm 0.03$ and is one order of magnitude higher than the rate constant determined in this study.[25] A likely reason the Suh and Hah catalyst reacts faster than **6e** is that their catalyst was a homogeneous catalyst where **6e** is a heterogeneous catalyst.

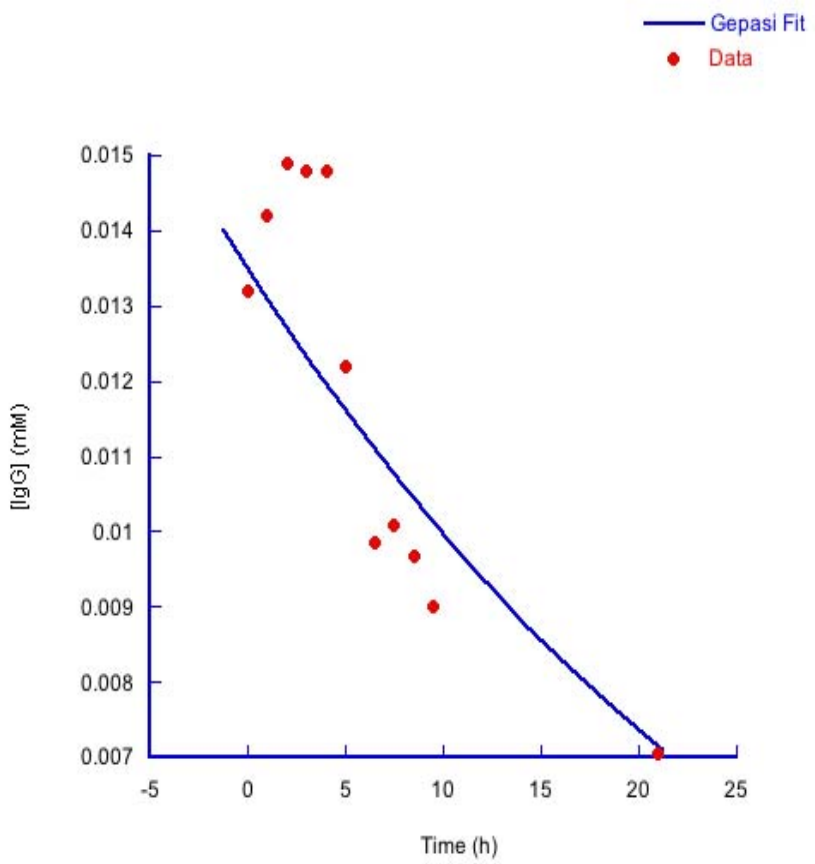

Figure 3.18 Gepasi results for **6e** Trial 1.

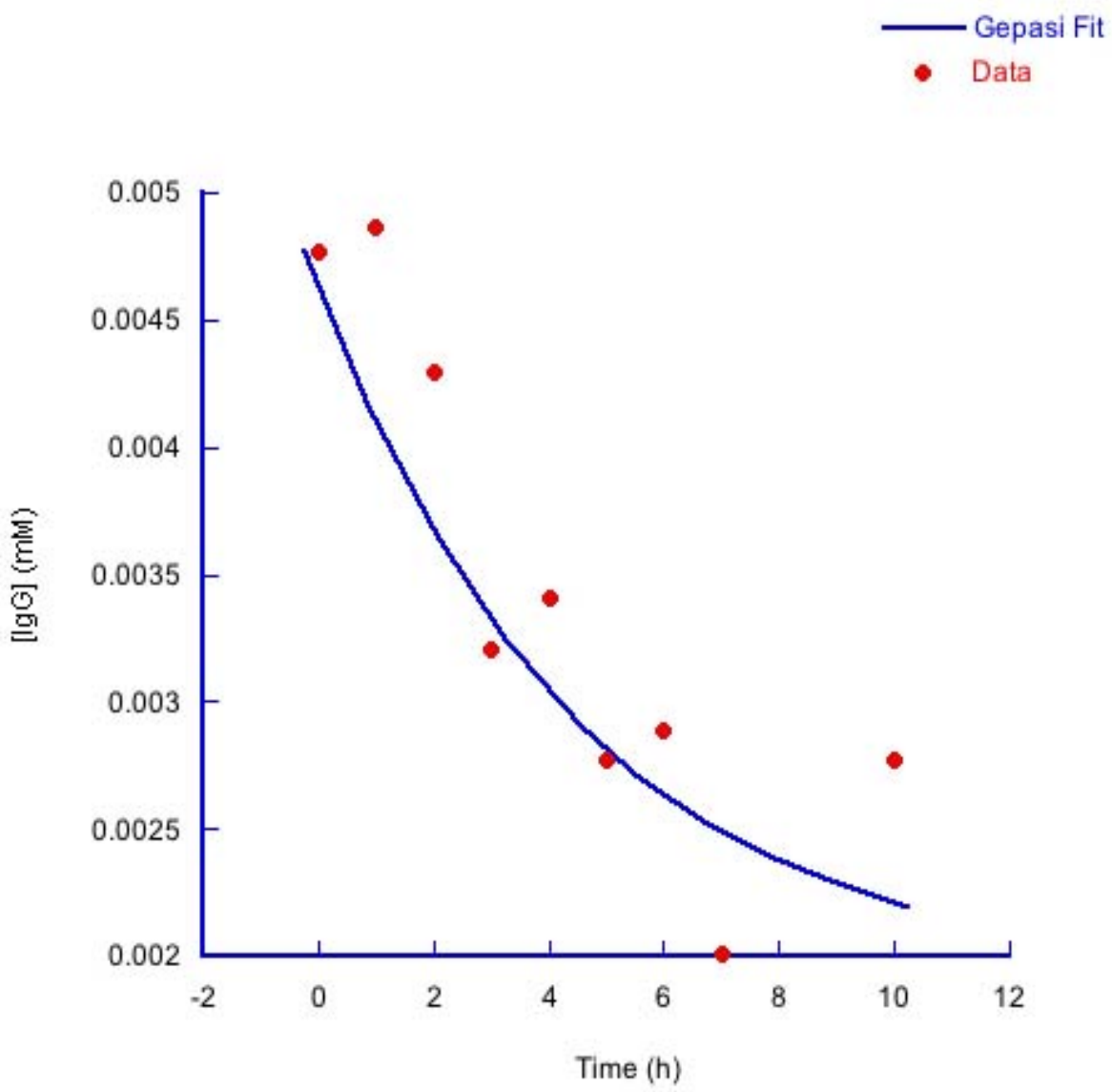

Figure 3.19 Gepasi results for **6e** Trial 3.

Summary

Dendrimers **6a-6e** were employed in kinetic studies of the cleavage of the peptide backbone of IgG. SDS-PAGE and Quantity-One software were used to monitor the reaction. Qualitative analysis shows that **6e, 6d** and **7** effectively cleave the backbone of the heavy chain of IgG. Dendrimers **6a, 6b,** and **6c** did not show catalytic activity under

the conditions of the experiment. An unbound salicylic acid derivative **1** also showed no activity. Gepasi Biochemical Kinetic Simulator software was used to calculate rate laws for **6e** and **6d**.

Experimental Procedures

General Procedures: General reagents were purchased from Aldrich, Sigma, Acros, and Bio-Rad chemical companies. Reagents were used as received without further purification.

General Procedure for IgG cleavage studies. IgG was dissolved in 0.5 M HEPES buffer solution. Deterium Oxide was used instead of water to minimize Fe^{+3} contamination. Concentration of the IgG solution was determined to be 8.8×10^{-3} mM by UV absorbance (ε=1.4 mL/(mg*cm)). Dendrimers **6a**-**6e** were lypholized to a gel consistency in separate 5 ml round bottom flasks. The flasks containing **6a**-**6e** and a flask containing the IgG solution were heated to 45 °C in an oil bath. The IgG solution and dendrimer were mixed such that if the dendrimer were in solution the concentration of SaI units would be 1.45 mM. Compounds **1** and **7** were weighed using a Mettler Micro Balance Model M5 and were also diluted with IgG solution to 1.45 mM. The mixtures were stirred using a carousel in a 45 °C oil bath. Aliquots of 20 μL were obtained approximately every hour for the first 8 hours with aliquots taken at 10, 12 and 22 hours. Aliquots were immediately placed in a 4 °C refrigerator.

The carousel is a device created using the motor of a rotary evaporator. The goal of the design was to spin four 5mL flasks in an oil bath simultaneously. The carousel

made the lengthy time commitment of the protein cleavage studies as productive as possible. Stir bars proved a significant source of Fe^{+3}, which binds strongly with dendrimers **6a-6e** deactivating catalytic capability. The dendrimers are heterogenous catalysts in the cleavage of the IgG peptide backbone. The reactions mixtures needed to be stirred in order to minimize localized high concentration of catalytic activity.

SDS-PAGE**.** After all aliquots were chilled, they were warmed to room temperature and 8 μL of SDS sample buffer was added to each. The sample buffer was composed of 25% glycerol, 0.156 M Tris-HCl, 5% SDS, 12.5% β-mercapto ethanol, and .0025% bromphenol blue. The aliquots were vortexed for 5 seconds, heated at 95 °C for 5 minutes, vortexed for 5 seconds, and centrifuged for 15 seconds. An amount of each aliquot (10 μL) was loaded onto a Bio-Rad precast Tris HCL 10% 15 well polyacrylamide gel. The gels were run using a Thermo Electron Corporation PRO 6000 power supply. The parameters of the power supply were set to 200 volts, 51 amps, and 6 watts. The running buffer was composed of 192 mM glycine, 0.1% SDS, and 24.8 mM Tris-HCL. When the dye front of the gels reached the bottom of the gels, the gels were removed from the running cell and soaked in 10% methanol and 7% acetic acid for 1 h. The gels were then stained in Sypro Ruby mini gel stain overnight and destained in 10% methanol and 7% acetic acid for 36 hours. The gels were then scanned using a Bio-Rad Molecular Imager FX. The gels were quantified using Quantity One software from Bio-Rad.

Quantity One Analysis. Each gel was scanned at 100 micrometers and subjected to a global background subtraction using the background box function. The rectangle

volume tool was used to label the individual bands of the heavy chain of IgG when the bands were uniform. In situations where the bands overlapped the volume freehand tool was used. None of the freehand bands were used in quantifying the gels. Given that the heavy chain could theoretically be cleaved into pieces roughly the same size as the light chain, the heavy chain results were the only results analyzed. A volume analysis report was generated for the selected bands.

Gepasi Analysis. The data from the volume analyses of **6d** and **6e** were used for Gepasi analysis. First the standard correction curve was generated. The experimental volumes of the standard bands were divided by the volume of S1 to afford percentage values for each band. These experimental percentages were plotted against the theoretical percentages from the serial dilution. A linear curve fit was applied to the data to give a standard error equation that would compensate for the experimental error in the standards. The volumes of the aliquot bands were adjusted by the standard error equation. The volume of S1 was adjusted with the standard error equation and then used to divide the concentration of S1 as determined by UV absorbance to give a ratio of volume : concentration. The volumes of the aliquot bands were converted to concentration in mM by the ratio of S1 band volume : corrected concentration. The concentrations and corresponding time (h) were loaded into the Gepasi Biochemical Kinetic Simulator to generate rate curves and rate laws using the catalytic kinetic activator model. The reaction models entered were IgG + Dendrimer -> 1000 fragments + dendrimer and 1 fragment + dendrimer -> inactive dendrimer. Both reactions were labeled mass action and irreversible. These models take into account the competitive inhibition of the

fragements with the dendrimer. The Gepasi fit was done using Multistart (Levenberg-Marquede) method.

CHAPTER FOUR

SUMMARY AND CONCLUSIONS

Generation 1-5 salicylic acid functionalized PPI dendrimers were synthesized and characterized by ^{1}H NMR, ^{13}C NMR, MALDI-TOF MS, and Micro-TOF MS. The Generation 5 salicylic acid functionalized PPI dendrimer was active as a catalyst in the cleavage of the peptide backbone of IgG. Generation 4 displayed weaker activity as a catalyst in the same reaction. Generations 1,2,3, and 5-nitrosalicylic acid displayed no catalytic activity. The activity was monitored by SDS-PAGE and quantified using Quantity One and Gepasi software. Generation 5 and 4 enhanced catalytic activity when compared to 5-nitrosalicylic acid. This catalytic dendrimer system is one of the few to display cooperativity between the endgroups of the dendrimer.

REFERENCES CITED

1. Cornils, B., Herrmann, W.A. Concepts in homogeneous catalysis: the industrial view. Journal of Catalysis, 2003, 216, 23-31.

2. Somorjai, G.A., McCrea, K. Roadmap for catalysis science in the 21st century: a personal view of building the future on past and present accomplishments. Applied Catalysis A: General, 2001, 222, 3-18.

3.Berzelius, J. Jaher-Bericht uber die Fortshritte der Physichen Wissenschaften, Vol. 15, H. Laupp, Tubingen, 1836.

4. Dijkstra, H.P., Van Klink, G.P.M., Van Koten, G. The Use of Ultra- and Nanofiltration Techniques in Homogeneous Catalyst Recycling. Acc. Chem. Res., 2002, 35, 798-810.

5. Schwartz, J. Alkane Activation by Oxide-Bound Oraganorhodium Complexs. Acc. Chem. Res., 1895, 18, 302-308.

6. Widegren, J.A., Finke, R. G. A review of the problem of distinguishing true homogeneous catalysis from soluble or other metal-particle heterogeneous catalysis under reducing conditions. J. Mol. Cat. A: Chem., 2003, 198, 317-341.

7. Suh, J. Synthetic Artificial Peptidases and Nucleases Using Macromolecular Catalytic Systems. Acc. Chem. Res., 2003, 36, 562-570.

8. Zhou, W., Liu, L., Breslow, R., Transamination by Polymeric Enzyme Mimics. Helvetica Chimica Acta. 2003, 86, 3560-3567.

9. Milovic, N.M., Kostic, N.M., Palladium (II) Complexes, as Synthetic Peptidases, Regioselectively Cleave the Second Peptide Bond “Upstream” from Methionine and Histidine Side Chains. JACS, 2002, 124, 4759-4769.

10. Hollfelder, F., Kirby, A.J., Tawfik, D.S., Efficient Catalysis of Proton Transfer by Synzymes. JACS, 1997, 119, 9578-9579,

11. Habicher, T., Diederich, F. Catalytic Dendrophanes as Enzymer Mimics: Synthesis, Binding Properties, Micropolarity Effect, and Catalytic Activity of Dendritic Tiazolio-cyclophanes. Helvetica Chimica Acta. 1999, 82, 1066-1095.

12. Newkone, G.R., Moorefield, C.N., and Vogtle, F. Dendrimers and Dendrons: Concepts, Syntheses, Applications. (Weinheim: Wiley-VGH) (2001).

13. Grayson, S.M., Frechet, J.M.J. Convergent Dendrons and Dendrimers: from Synthesis to Application. Chem. Rev., 2001, 101, 3819-3867.

14. Bosman, A.W., Janssen, H.M., Meijer, E.W. About Dendrimers: Structure, Physical Properties, and Applications. Chem. Rev., 1999, 99, 1665-1688.

15. Buhleier, E., Wehner, W., Vogtle. Syntheis, 1978, 155-158.

16. de Brabander-van den Berg, E.M.M., Meijer, E.W. Poly(propylene imine) Dendrimers: Large-Scale Synthesis by Hetereogeneously Catalyzed Hydrogenations. Angew. Chem. Int. Ed. Engl. 1993, 32, 1308-1311.

17. de Brabander-van den Berg, E.M.M., Nijen-huis, A., Mue, M., Keulen, J., Reintjens, R., Frijns, F.T., Wal, S.V.D., Castelijns, M., Put, J., Meijer, E.W. Large-Scale Production of Polypropylenimine Dendrimers. Macromol. Symp. 1994, 77, 51-62.

18. Astrac, D., Heuze, K., Gatard, S., Nlate, S., Plault, L., Mery, D. Metallodendritic Catalysis for Redox and C-C Bond Formation Reactions. Adv. Synth. Catal., 2005, 347, 329-338.

19. van de Coevering, R., Klein Gebbink, R.J.M., van Koten, G. Soluble organic supports for the non-covalent immobilization of homogeneous catalysts; modular approaches towards sustainable catalysts. Prog. Polym. Sci., 2005, 30, 474-490.

20. Frechet, J.M.J. Dendrimers and Other Dendritic Macromolecules: From Building Blocks to Functional Assemblies in Nanoscience and Nanotechnology. J. Polym. Sci. Part A: Polym. Chem., 2003, 41, 3713-3725.

21. van Heerbeek, R., Kamer, P.C.J., van Leeuwen, P.W.N.M., Reek, J.N.H. Dendrimers as Support for Recoverable Catalysts and Reagents. Chem. Rev., 2002, 102, 3717-3756.

22.Twyman, L.J., King, A.S.H., Martin, I.K. Catalysis inside dendrimers. Chem. Soc. Rev., 2002, 31, 69-82.

23. Twyman, L.J., King, A.S.H. Catalysis peripherally functionalized dendrimers. J. Chem. Res., 2002, 2, 201-243.

24. Liang, C., Frechet, J.M.J. Applying key concepts from nature: transition state stabilization, pre-concentration and cooperativity effects in dendritic biomimetics. Prog. Polym. Sci., 2005, 30, 385-402.

25. Suh, J.S., Hah, S.S. Organic Artificial Proteinase with Active Site Comprising Three Salicylate Residues. JACS, 1998, 120, 10088-10093.

26. Samuelson, L.E., Sebby, K.B., Walter, E.D., Singel, D.J., Cloninger, M.J. EPR and affinity studies of mannose-TEMPO functionalized dendrimers. Organic & Biomolecular Chemistry, 2004, 21, 3075-3079.

27. Woller, E.K., Walter, E.D., Morgan, J.R., Singel, D.J., Cloninger, M.J. Altering the strength of lectin binding interactions and controlling the amount of lectin clustering using mannose/hydroxyl-functionalized dendrimers. JACS, 2003, 29, 8820-8826.

28. Woller, E.K., Cloninger, M.J. Mannose functionalized of a sixth generation dendrimer. Biomacromolecules, 2001, 2, 1052-1054.

29. Woller, E.K., Cloninger, M.J. The lectin-binding properties of six generations of mannose-functionalized dendrimers. Organic Letters, 2002, 4, 7-10.

30. Kakigami, T., Baba, K., Usui, T. A Facile Synthesis of Methyl 5-Amino-6-chloro-2H-1-benzopyran-8-carboxylate derivatives. Heterocycles, 1998, 48, 1998.

31. Wessely, F., Benedikt, K., Benger, H. Zur Synthese der Aminosalicylsauren. Monatsheften Fur Chemie. 1949. 80, 197-199.

32.Suh, J., Park, H.S. Fe (III) Sequestering Agents Built on Poly(ethylenimine) through Crosslinkage of Three Molecules of a Salicylate Derivative Preassembled by Fe (III) Ion. J. Polym. Sci. Part A: Polym. Chem., 1997, 35, 1197-1210.

33. Hoye, T.R., Eklov, B.M., Voloshin, M. No-D NMR Spectroscopy as a Convenient Method for Titering Organolithium (RLi), RMGX, and LDA Solutions. Org. Lett., 2004, 6, 2567-2570.

34. Hoye, T.R., Eklov, B.M., Voloshin, M. No-D NMR (No-Deterium Proton NMR) Spectroscopy: A Simple yet Powerful Method for Analyzing Reaction and Reagent Solutions. Org. Lett., 2004, 6, 953-956.

35. Bodnar, I., Silva, A.S., Deithcher, R.W., Weisman, N.E., Kim, Y.H., Wagner, N.J. Structure and Rheology of Hyperbranched and Dendritic Plolymers. I. Modification and Characterization of Poly(propyleneimine) Dendrimers with Acetyl Groupls. J. Poly. Sci. Part B: Polym. Physics, 2000, 38, 857-873.

36. Busch, K.L. Mechanisms of MALDI. Spectroscopy, 1999, 10, 14-19.